Biosystems, Foster City, CA, USA) was used for PCR amplification. The amplification program used was 35 cycles of 30 s at 94°C, 30 s at 64°C, and 40 s at 72°C, with a final incubation of 7 min at 72°C.

Flow cytometry and cell sorting

Cultured cells were incubated with enzyme-free Hank's-based Cell Dissociation Buffer (Invitrogen) for 30 min at 37°C and gently dissociated into single cells. The cells were then washed with PBS twice, probed with biotinylated-SM/C-2.6 (23) antibody for 15 min at room temperature, and stained with phycoerythrin-conjugated strepavidin (12-4312; eBioscience, San Diego, CA, USA) for 15 min at room temperature. Dead cells were excluded from the plots based on propidium iodide staining (Sigma), and SM/C-2.6-positive cells were collected using a FACS Vantage instrument (Becton Dickinson, San Jose, CA, USA). Sorted cells were plated (1×10^4 cells/well) with differentiation medium in 96-well plates (Falcon) coated with Matrigel (008504; BD Bioscience). The medium was changed every 5 d, and 7 d after plating the cultured cells were analyzed.

Intramuscular cell transplantation (primary transplantation)

Recipient mice were injected with 50 μl of 10 μM cardiotoxin (CTX; Latoxan, Valence, France) (30) in the LTA muscle 24 h before transplantation (31). CTX is a myotoxin that destroys myofibers, but not satellite cells, and leaves the basal lamina and microcirculation intact. Since proliferation of host myogenic cells may prevent the incorporation of transplanted cells, recipient mdx mice (15) received 8 cGy of systemic irradiation (32) 12 h before transplantation to block muscle repair by endogenous cells. An average of 4.53×10^4 ES-derived SM/C-2.6-positive or -negative cells were washed twice with 500 μl of PBS, resuspended in 20 μl of DMEM, and injected into the LTA muscle of recipient mdx mice using an allergy syringe (Becton Dickinson). Mdx mice, which are derived from the CL/B16 strain, were used as the recipient mice in all experiments. Similarly, D3 ES cells, which are derived from the 129X1/SvJ ES cells, were used in all experiments. The major histocompatibility complex (MHC) of mdx mouse and D3 cells are very similar, both possessing type *b* MHC H2 haplotypes. All animal-handling procedures followed the Guild for the Care and Use of Laboratory Animals published by the U.S. National Institutes of Health (NIH Publication No. 85-23, revised 1996) and the Guidelines of the Animal Research Committee of the Graduate School of Medicine, Kyoto University.

Secondary transplantation

The LTA muscles of recipient mice were collected 8 wk after the primary transplantation. The muscles were minced and digested into single cells with 0.5% collagenase type I (lot S4D7301; Worthington Biochemical Corp., Lakewood, NJ, USA). After washing with PBS and filtration through a 100 μm filter, Pax7-positive cells were sorted by FACS using the SM/C-2.6 antibody. SM/C-2.6-positive cells (200 cells/mouse) were injected into preinjured LTA muscles of secondary recipient mice. The LTA muscles were analyzed 8 wk after transplantation.

Isolation and immunostaining of single fibers

To detect muscle satellite cells attaching to single fibers with Pax7, muscle fibers from the LTA muscle of recipient mice were prepared essentially according to the method of Bischoff in Rosenblatt *et al.* (33). Briefly, dissected muscles were incubated in DMEM containing 0.5% type I collagenase (Worthington) at 37°C for 90 min. The tissue was then transferred to prewarmed DMEM containing 10% FBS. The tissue was gently dissociated into single fibers by trituration with a fire-polished wide-mouth Pasteur pipette. Fibers were transferred to a Matrigel-coated 60 mm culture dish (Falcon) and fixed in 4% PFA for 5 min at room temperature. Fibers were permeabilized with 0.1% Triton X-100 in PBS for 10 min, and nonspecific binding was blocked by incubation in 5% skim milk for 10 min at room temperature. Primary mouse monoclonal antibodies against mouse Pax7 were applied for 12 h at 4°C. Antibodies were detected using the secondary antibodies described above.

Statistics

Data are presented as means ± SD. For comparison of the numbers of MHC and Pax7-positive cells in the sorted SM/C-2.6-positive and -negative fractions and the numbers of GFP-positive muscle fascicles and GFP/Pax7-double-positive cells in reinjured and noninjured groups, the unpaired Student's t test was used, and a value of $P < 0.05$ was considered to be statistically significant.

RESULTS

Myogenic lineage cells are effectively induced from mES cells *in vitro*

EBs were formed in hanging drop cultures for 3 d followed by an additional 3 d in suspension cultures (**Fig. 1*A***). These EBs were then plated onto Matrigel-coated 48-well plates in differentiation medium, which contained 5% HS. This culture method is a modified version of the classical ES cell differentiation method (25) and the skeletal muscle single fiber culture method (33). After plating, EBs quickly attached to the bottom of the coated dishes, and spindle-shaped fibers appeared surrounding the EBs by the seventh day of plating (d 3+3+7; Fig. 1*B*). As these spindle fibers grew, they began to fuse with each other, forming thick multinucleated fibers resembling skeletal myofibers (Fig. 1*C, D*). At the same time we observed spontaneous contractions by the fibers (Supplemental Videos 1 and 2), a trait commonly seen in cultured skeletal muscle fibers. Immunostaining showed that these fused fibers were positive for skeletal-muscle-specific MHC (Fig. 1*E*). Furthermore, cells expressing muscle regulatory factor (MRF) proteins, including Pax7 (Fig. 1*F*), Myf5 (Fig. 1*G*), MyoD (Fig. 1*H*), and myogenin (Fig. 1*I*) were observed. On d 3 + 3 + 14, the average number of MHC-positive wells was 73.6 ± 5.8% (n=144). In all the MHC-positive wells, cells expressing Pax7, an essential transcription factor in satellite cells, were also observed. Double staining for Pax7 and MyoD confirmed the existence of cells staining for Pax7 alone, indicating the presence of quiescent-state satellite cells (34) within the culture (Supplemental Fig. 1). Next, the time course of MRF expression was examined by RT-PCR (Fig. 1*J*). Expression of Pax3 and Pax7 both peaked on d 3 + 3 +

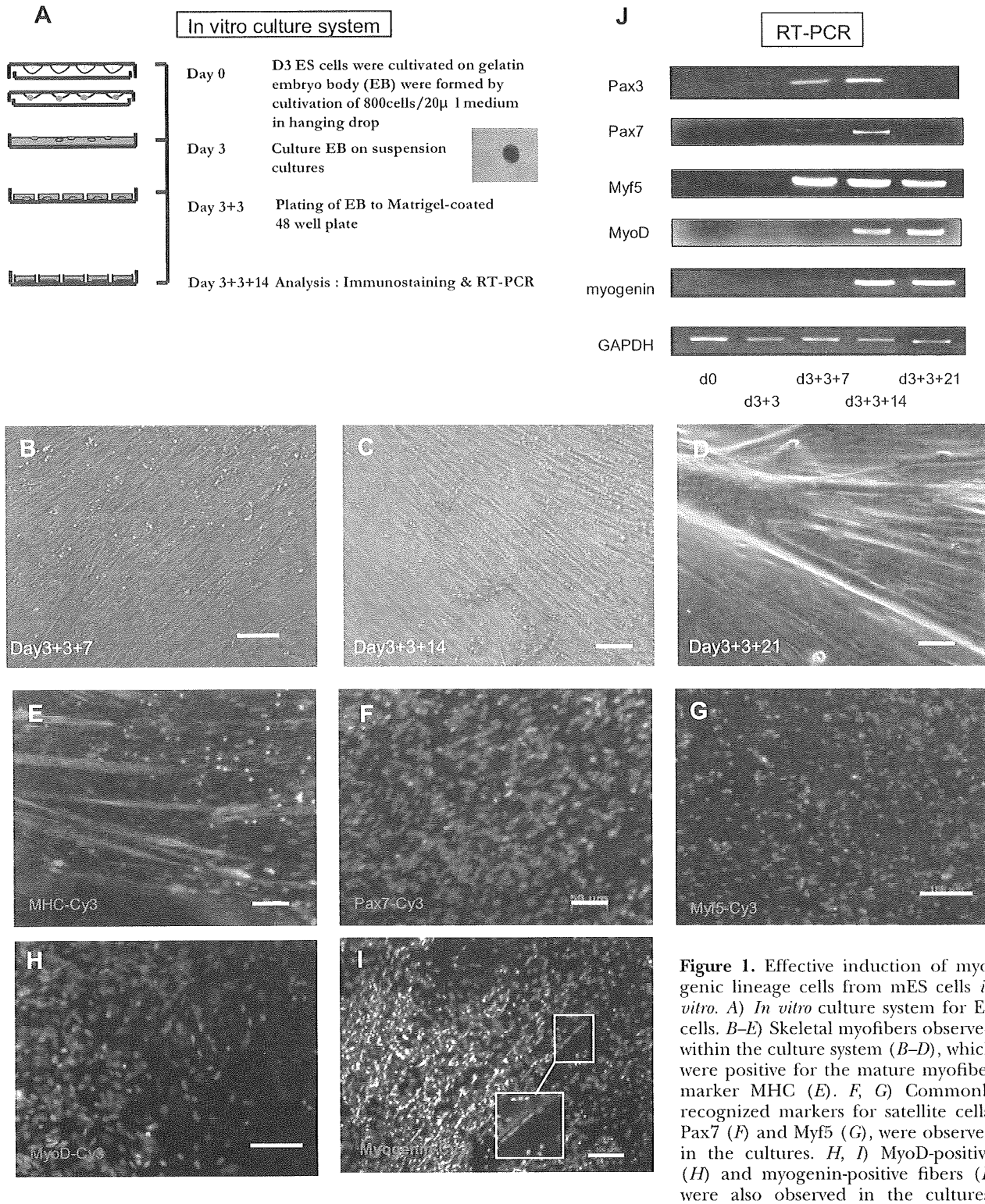

Figure 1. Effective induction of myogenic lineage cells from mES cells *in vitro*. *A*) *In vitro* culture system for ES cells. *B–E*) Skeletal myofibers observed within the culture system (*B–D*), which were positive for the mature myofiber marker MHC (*E*). *F, G*) Commonly recognized markers for satellite cells, Pax7 (*F*) and Myf5 (*G*), were observed in the cultures. *H, I*) MyoD-positive (*H*) and myogenin-positive fibers (*I*) were also observed in the cultures. White boxes indicate multinucleated myotubes (*I*). *J*) RT- PCR expression of MRFs including Pax3, Pax7, Myf5, MyoD, and myogenin in ES cells in our novel culture system at d 0, 3 + 3, 3 + 3 + 7, 3 + 3 + 14, and 3 + 3 + 21. Scale bars = 50 μm (*A–F*); 100 μm (*G–I*).

14, but Myf5, MyoD, and myogenin continued to be expressed after d 3 + 3 + 14.

Thus, using Matrigel plates and differentiation medium containing HS, myogenic lineages including Pax7-positive satellite-like cells were successfully induced from mES cells.

A novel antibody, SM/C-2.6, can enrich for Pax7-positive satellite-like cells derived from ES cells

To examine the characteristics of ES-derived Pax7-positive satellite-like cells, we needed to isolate these cells from the culture. Since Pax7 is a nuclear protein rather than a

surface marker, anti-Pax7 antibodies cannot be used for living cell separation by FACS. Therefore, a novel antibody, SM/C-2.6 (23), was used to detect satellite cells. SM/C-2.6 detects quiescent adult mouse satellite cells, as well as satellite cells in neonatal muscle tissue, as determined by immunostaining (Supplemental Fig. 2). RT-PCR confirmed that sorted SM/C-2.6-positive cells expressed Pax3, Pax7, Myf5, and c-met, whereas sorted SM/C-2.6-negative cells did not (Supplemental Fig. 3). Thus, the SM/C-2.6 antibody was shown to be useful for isolating living satellite cells by FACS.

We collected all the differentiated ES cells (1×10^6 cells) from cultures on d 3 + 3 + 14. FACS analysis using the SM/C-2.6 antibody showed that 15.7% of the cells were SM/C-2.6 positive (**Fig. 2*A***). RT-PCR analysis revealed that sorted SM/C-2.6-positive cells strongly expressed Pax3, Pax7, Myf5, c-met, and M-cadherin (Fig. 2*B*). Using a cytospin preparation of sorted SM/C-2.6-positive cells, we also confirmed the expression of M-cadherin (Fig. 2*C*) and Pax7 (Fig. 2*D;* 70.7±16.5% and 59.9±1.1% positive, respectively); only 2.3 ± 0.49% of the sorted SM/C-2.6-negative cells expressed M-cadherin, and 2.7 ± 0.1% expressed Pax7. Thus, the SM/C-2.6 antibody could enrich for satellite-like cells derived from mES cells *in vitro.*

ES-derived satellite-like cells have strong myogenic potential *in vitro*

To evaluate the myogenic potential of ES-derived SM/C-2.6-positive satellite-like cells *in vitro,* both SM/C-2.6-positive and -negative cells were sorted by FACS and plated in 96-well Matrigel-coated plates (see Fig. 4A). One week after cultivation, the number of muscle fibers in the wells was assessed. Although there were fibroblast-like and endothelium-like cells, MHC-positive fibers (787.3±123.7/well, 10.7±0.8% of the total cells per well, n=3) and Pax7-positive cells (222±81.4/well, 2.9±1.1% of the total cells per well, n=9) were observed in the SM/C-2.6-positive wells. In contrast, very few MHC-positive fibers (8.75±32.6/well, n=15; 0.12±0.46%) or Pax7-positive cells (2.6±2.0/well, n=8; 0.03±0.01%) were seen in the SM/C-2.6-negative wells

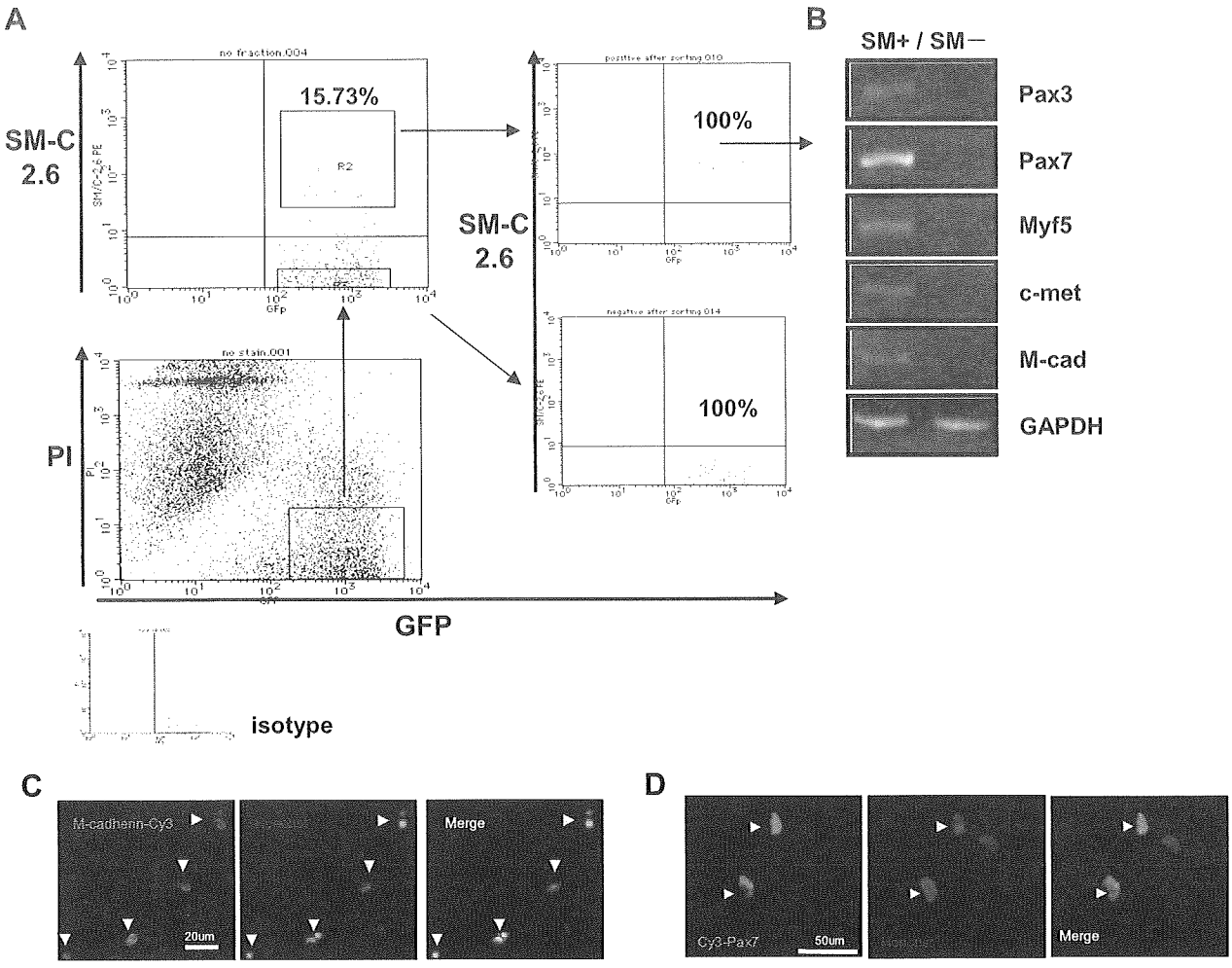

Figure 2. A novel antibody, SM/C-2.6, can enrich Pax7-positive satellite-like cells derived from ES cells. *A*) FACS data of cultured ES cells at d 3 + 3 + 14 indicate that 15.7% of total cultured cells are SM/C-2.6-positive cells. *B*) RT-PCR of the SM/C-2.6-positive fraction showed strong expression of Pax3, Pax7, Myf5, c-met, and M-cadherin. Immunostaining of a cytospin preparation of the sorted SM/C-2.6-positive cells showed that these cells were positive for M-cadherin (*C*), and Pax7 (*D*) (white arrowheads). Scale bars = 20 μm (*C*); 50 μm (*D*).

(both $P<0.05$; **Fig. 3**). Thus, ES-derived satellite-like cells isolated using the SM/C-2.6 antibody possess strong myogenic potential *in vitro*.

Damaged muscle can be repaired by transplantation of ES-derived satellite-like cells

To examine the myogenic potential of ES-derived satellite-like cells *in vivo*, SM/C-2.6-positive and -negative cells were transplanted into conditioned mdx mice (15). The LTA muscles of recipient mdx mice were preinjured with CTX (primary injury; ref. 30) 24 h prior to transplantation, and mice were exposed to 8 cGy of γ-irradiation (whole body) 12 h prior to transplantation (**Fig. 4A**). GFP-positive ES cells were used as donor cells in this experiment. GFP^+ES-derived SM/C-2.6-positive and -negative cells were directly injected into the predamaged LTA muscles. The recipient mice were analyzed 3 wk post-transplantation. By fluorescence stereomicroscopy, GFP-positive tissues were clearly observed within the LTA muscles injected with SM/C-2.6-positive cells (Fig. 4*B* and **Table 1**). In contrast, no GFP-positive tissue was observed in muscles injected with SM/C-2.6-negative cells (Fig. 4*C*). These GFP-positive tissues were further confirmed by diaminobenzidine staining using anti-GFP and a peroxidase-conjugated secondary antibody (Supplemental Fig. 4) to exclude the possibility of autofluorescence of the muscle tissues. Immunostaining with anti-MHC confirmed that these GFP-positive tissues were mature skeletal myofibers (Fig. 4*D*). In addition, GFP/Pax7 double-positive cells were observed within the LTA muscles of the recipient mice (Fig. 4*E* and Supplemental Fig. 5) and in isolated single fibers (Fig. 4*F* and Table 1). The GFP-positive cells were also confirmed to be positive for other satellite cell markers such as Myf5 and M-cadherin (Supplemental Figs. 6 and 7). These GFP/Pax7-double-positive cells were located along the periphery of the muscle fascicle. With laminin immunostaining we verified that the location of the GFP-positive mononuclear cells was between the basal lamina and the muscle cell plasma membrane, a location consistent with the anatomical definition of satellite cells

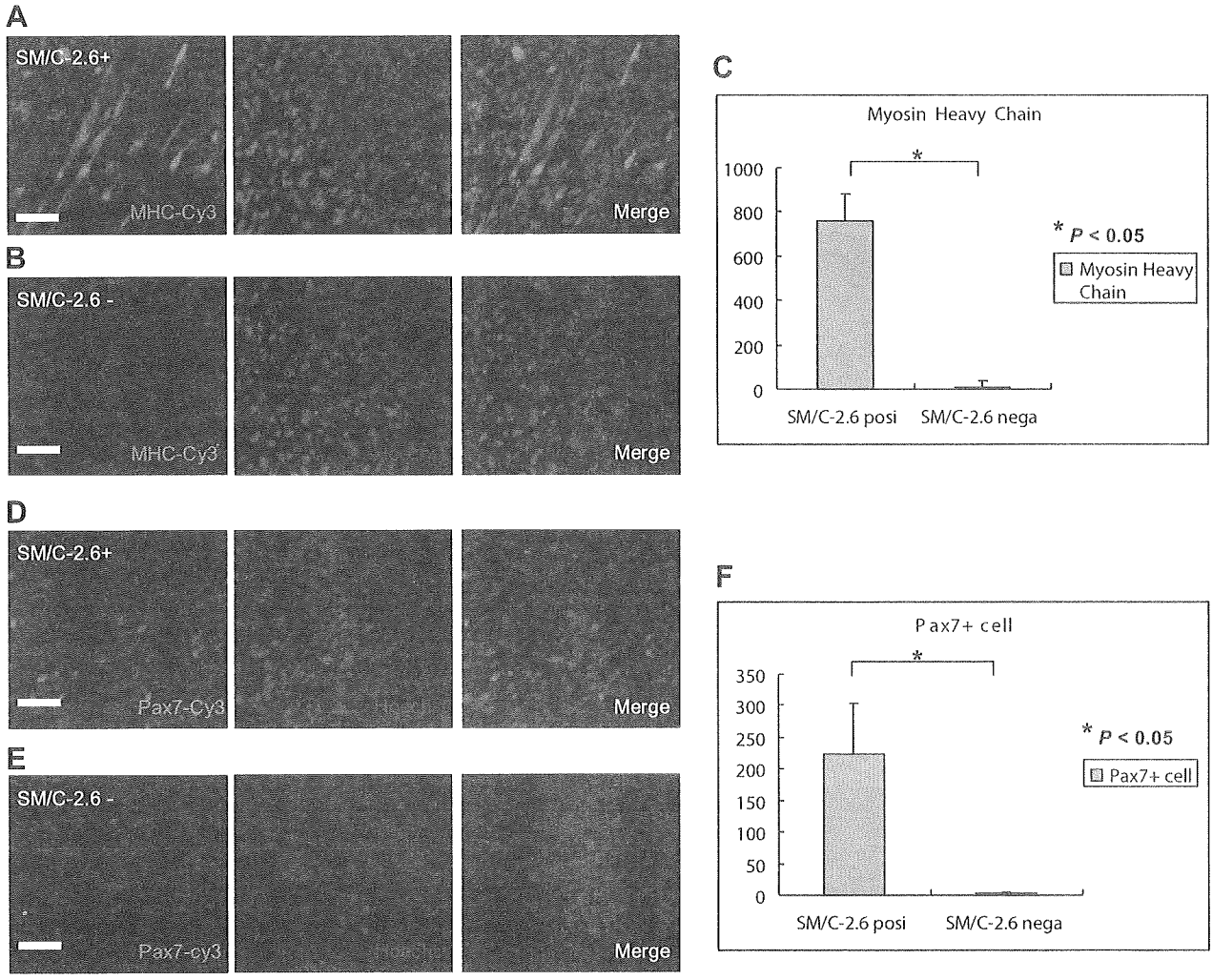

Figure 3. ES-derived satellite-like cells have strong myogenic potential *in vitro*. Immunostaining detected an abundant number of MHC-positive fibers and Pax7-positive cells in SM/C-2.6-positive cell culture (*A*, *D*) but not SM/C-2.6-negative cells (*B*, *E*) after 1 wk in culture. Scale bars = 50 μm. Significant differences were observed in the number of MHC-positive fibers and Pax7-positive cells per well between sorted SM/C-2.6-positive and -negative cell cultures (*C*, *F*).

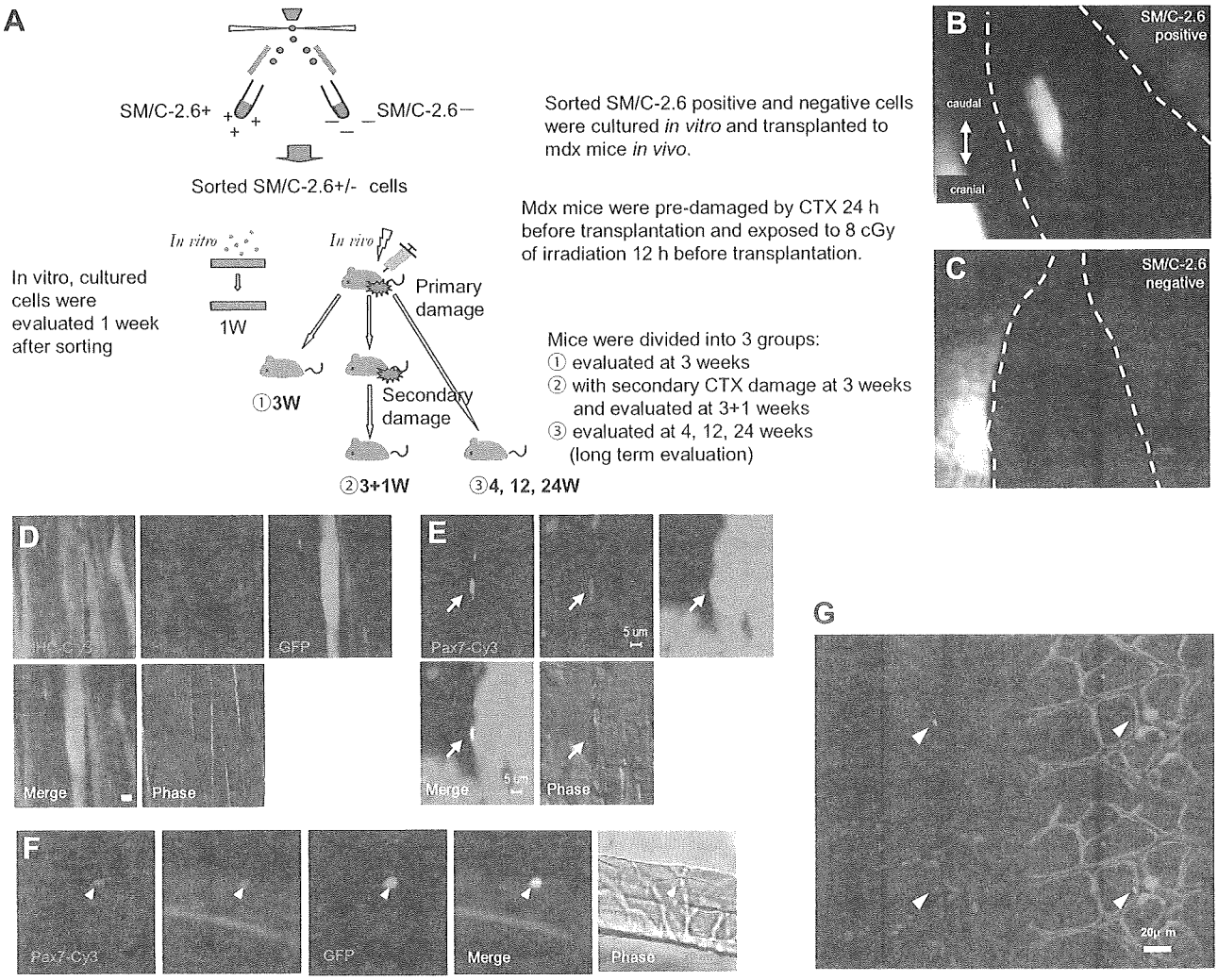

Figure 4. ES-derived satellite-like cells can repair damaged muscle *in vivo*. *A*) Methods for *in vitro* and *in vivo* analysis of sorted SM/C-2.6-positive and -negative cells derived from mES cells. *B, C*) ES-derived GFP-positive tissue engrafted to the LTA muscle of a recipient mouse that received SM/C-2.6-positive cells (*B*) but SM/C-2.6-negative cells (*C*). *D*) Grafted GFP-positive tissues were histologically MHC positive. *E*) GFP/Pax7-double-positive cells were observed in mice that received SM/C-2.6-positive cells by anti-Pax7 immunostaining. *F*) GFP/Pax7-double-positive cells were also confirmed by immunostaining of isolated single fibers. *G*) Laminin immunostaining indicated that the GFP-positive cells were located between the basal lamina and the muscle cell plasma membrane, which is consistent with the anatomical definition of muscle satellite cells. Scale bars = 1 mm (*B, C*); 15 μm (*D*); 5 μm (*E*); 20 μm (*F, G*).

(Fig. 4*G*). In contrast, in mice transplanted with SM/C-2.6-negative cells, GFP-positive tissues were rarely observed, and none of the GFP-positive cells were positive for skeletal MHC. H&E staining indicated that these GFP-positive tissues were surrounded by inflammatory cells (Supplemental Fig. 8), suggesting that these nonmyogenic tissues may undergo phagocytosis. These results demonstrate that ES-derived SM/C-2.6-positive satellite-like cells could be engrafted *in vivo* and repair damaged muscle tissues of the host.

Engrafted ES-derived satellite-like cells function as satellite cells following muscle damage

Muscle satellite cells are generally considered to be self-renewing monopotent stem cells that differentiate into myoblasts and myofibers to repair damaged skeletal muscles. To determine whether these engrafted GFP$^+$ES-derived satellite-like cells are functional stem cells, we injured the LTA muscle of primary recipient mice 3 wk after primary transplantation with GFP$^+$SM/C-2.6-positive cells. This experiment let us assess the ability of satellite-like cells to repair damaged muscle fibers and self-renew *in vivo* (14). The LTA muscles were removed and analyzed 1 wk after the secondary injury (reinjured group). Mice that were initially injected with GFP$^+$SM/C-2.6-positive cells without a second injury were used as a control (nonreinjured group). These control mice were analyzed 3 or 4 wk after transplantation (Fig. 4*A*). GFP-positive muscle fascicles were counted in sections of both reinjured and nonreinjured muscle (**Fig. 5*A, B***). In the reinjured group 461.7 ± 117.4 (n=6; per view, ×100) GFP-positive muscle fascicles were observed. In comparison, only 136.7 ± 27.9 (n=4) and 168.7 ± 72.9 (n=6; per view, ×100) GFP-positive muscle fascicles were evident in

TABLE 1. *Transplantation of reinjured and nonreinjured mice and long-term evaluation*

Group	TA with GFP$^+$ fascicles [n(%)][a]	Mouse	Cells/TA injected (n)	GFP$^+$ fascicles/TA (avg)[b]	GFP$^+$/Pax7$^+$ cells/TA (avg)[c]	Engraftment efficiency
SM/C-2.6$^+$						
3W	4/8 (50%)	1	1.75×10^4	125.3	5.3	
		2	3.5×10^4	111.1	7.1	
		3	5×10^4	134.2	5.1	
		4	8×10^4	176.1	4.2	
Mean			$4.5 \pm 2.6 \times 10^4$	136.7 ± 27.0	5.4 ± 1.2	0.30%
4W	6/9 (66.67%)	1	2×10^4	77.3	6.1	
		2	1.3×10^5	153.2	4.6	
		3	5×10^4	163.1	6.8	
		4	3.5×10^4	168.9	5.1	
		5	8×10^4	281.1	7.2	
		6	1.75×10^4	169.4	6.2	
Mean			$3.6 \pm 2.5 \times 10^4$	168.7 ± 72.9	6 ± 1	0.47%
3 + 1W	6/8 (75%)	1	2×10^4	581.2	11.2	
		2	1.3×10^5	370.3	11.5	
		3	5×10^4	586.6	10.1	
		4	3.5×10^4	486.6	5.9	
		5	8×10^4	347.1	15.3	
		6	1.75×10^4	542.9	10.8	
Mean			$5.5 \pm 4.3 \times 10^4$	461.7 ± 117.3	10.8 ± 3	0.84%
12W	3/5 (60%)	1	2×10^4	391.5	9.7	
		2	5×10^4	266	9.3	
		3	8×10^4	280.2	6	
Mean			$5 \pm 3 \times 10^4$	312.6 ± 68.7	8.3 ± 2	0.59%
24W	1/2 (50%)	1	2×10^4	58.62	3.45	
Mean			2×10^4	58.62	3.45	0.20%
SM/C-2.6$^-$						
3W	0/8 (0%)	1–8	$1–8 \times 10^4$	0	0	0%
4W	0/9 (0%)	1–9	$1.3–8 \times 10^4$	0	0	0%
3 + 1W	0/8 (0%)	1–8	$1.75–13 \times 10^4$	0	0	0%
12W	0/5 (0%)	1–8	$2–8 \times 10^4$	0	0	0%
24W	0/2 (0%)	1–2	2×10^4	0	0	0%

Serial transplantation

	Primary transplantation		Secondary transplantation		
Mouse	Cells injected	Collected GFP$^+$ cells/TA	Cells injected	GFP$^+$ fascicles/TA	Engraftment efficiency
1	2×10^4	3253	200	29.3	14.7%
2	2×10^4	2277	200	28.6	14.3%
Mean	2×10^4	2765	200	29 ± 0.5	14.5%

TA, tibialis anterior; 3W, nonreinjured group analyzed 3 wk after cell transplantation; 4W, nonreinjured group analyzed 4 wk after cell transplantation; 3 + 1W, reinjured group reinjured 3 wk after cell transplantation and analyzed 1 wk after reinjury; 12W, long-term engraftment evaluation analyzed 12 wk after cell transplantation; 24W, long-term engraftment evaluation analyzed 24 wk after cell transplantation. [a]Percentage of TA that had engrafted with GFP$^+$ fibers was calculated as number of TAs with GFP$^+$ fibers/total TAs injected with cells. [b]Average determined from number of GFP$^+$ muscle fascicles counted per field at ×100 in 10 fields. [c]Average determined from number of GFP$^+$/Pax7+ cells counted per field at ×100 in 10 fields.

the nonreinjured groups at 3 and 4 wk, respectively, after transplantation (Fig. 5*B* and Table 1). Furthermore, we also observed that many GFP-positive muscle fibers had a typical central nucleus in the reinjured group (Fig. 5*C*), indicating regenerating muscle fibers. Taken together, these results suggest that these GFP-positive muscle tubes were freshly regenerated by the engrafted GFP$^+$ ES-derived satellite-like cells in response to the second injury. Surprisingly, immunostaining with anti-Pax7 revealed an increase in number of GFP/Pax7-double-positive cells in the reinjured group (10.8±3.0/view compared to 5.4±1.2, and 6.0±1.0 in the nonreinjured group; Fig. 5*D* and Table 1). This result strongly suggests that engrafted ES-derived satellite-like cells not only self-renewed but also expanded in number, possibly replacing the recipient satellite cells lost because of excessive repair of skeletal muscle in response to the second injury.

ES-derived satellite-like cells are capable of long-term engraftment in recipient muscles

Long-term engraftment is an important characteristic of self-renewing stem cells. If these ES-derived satellite-

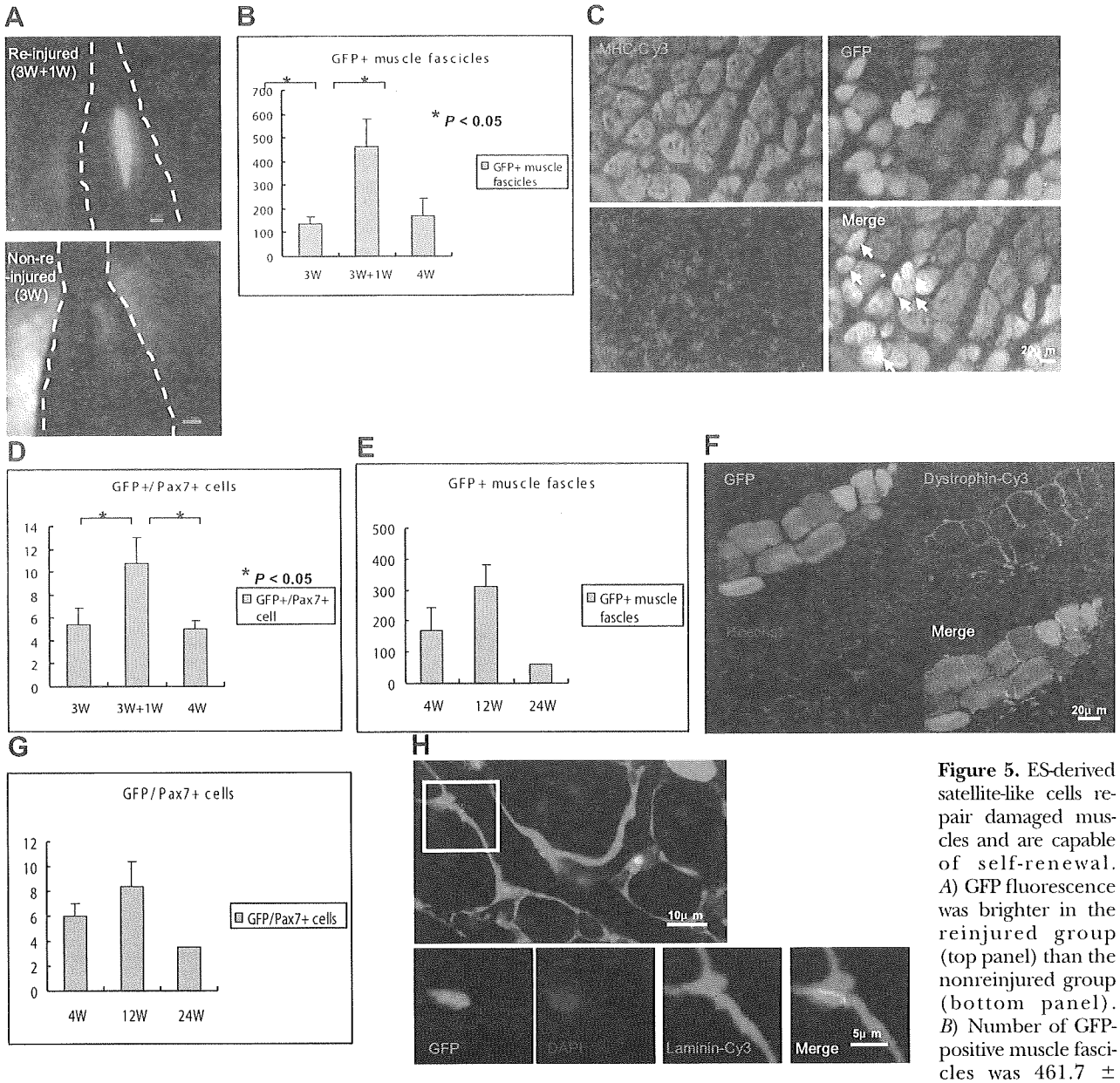

Figure 5. ES-derived satellite-like cells repair damaged muscles and are capable of self-renewal. *A*) GFP fluorescence was brighter in the reinjured group (top panel) than the nonreinjured group (bottom panel). *B*) Number of GFP-positive muscle fascicles was 461.7 ± 117.3 in the reinjured group (3W+1W) and 136.7 ± 27.9 and 168.7 ± 72.9 in the nonreinjured group at 3 wk (3W) and 4 wk (4W), respectively. *C*) GFP-positive fibers were confirmed to be MHC positive and contained central nuclei (arrows). *D*) Number of GFP/Pax7-double-positive cells also increased significantly in the reinjured group (10.8±3.0 cells at 3W+1W) compared to the nonreinjured group (5.4±1.2 and 6.0±1.0 at 3W and 4W, respectively). *E*) In long-term evaluations, number of GFP-positive muscle fascicles at 12 wk (12W) increased relative to number at 4 wk after transplantation [312.6±68.7 (n=3) *vs.* 168.7±72.9]. However, a decrease was observed at 24 wk (58.6; n=1). *F*) Immunostaining showed dystrophin (red) surrounding the donor-derived GFP-positive fibers (green), 24 wk after transplantation of SM/C-2.6-positive cells. *G*) Results similar to *E* were observed with the number of GFP/Pax7-double-positive cells. *H*) A GFP-positive cell beneath the basal lamina was observed. Scale bars = 1 mm (*A*); 20 μm (*C*); 20 μm (*F*); 10 μm (*H*, top panel); 5 μm (*H*, bottom panels).

like cells function as normal stem cells in skeletal muscle, they should be able to reside within the tissue for long periods of time and undergo asymmetric cell divisions to maintain the number of satellite cells and to generate muscle fibers. To examine this stem cell function, we analyzed the recipient mice at 4, 12, and 24 wk after transplantation. Intriguingly, in the LTA muscle of mdx mice transplanted with SM/C-2.6-positive cells, the number of GFP-positive fascicles at 12 wk increased over that at 4 wk [12.6±68.7 (n=3) *vs.* 168.7±72.9; Fig. 5*E*] but decreased by 24 wk (58.6; n=1). These engrafted GFP-positive tissues were confirmed to be MHC positive through immunostaining (Supplemental Fig. 9), and surrounding these GFP-positive fibers, dystrophin was observed (Fig. 5*F*). The numbers of GFP/Pax7-double-positive cells were maintained from week 4 to week 24 (Fig. 5*G*, Table 1, and Supplemental Fig. 10) and the location of GFP-positive cells under the basal lamina meets the anatomical definition of satellite cells (Fig. 5*H*). No teratomas were

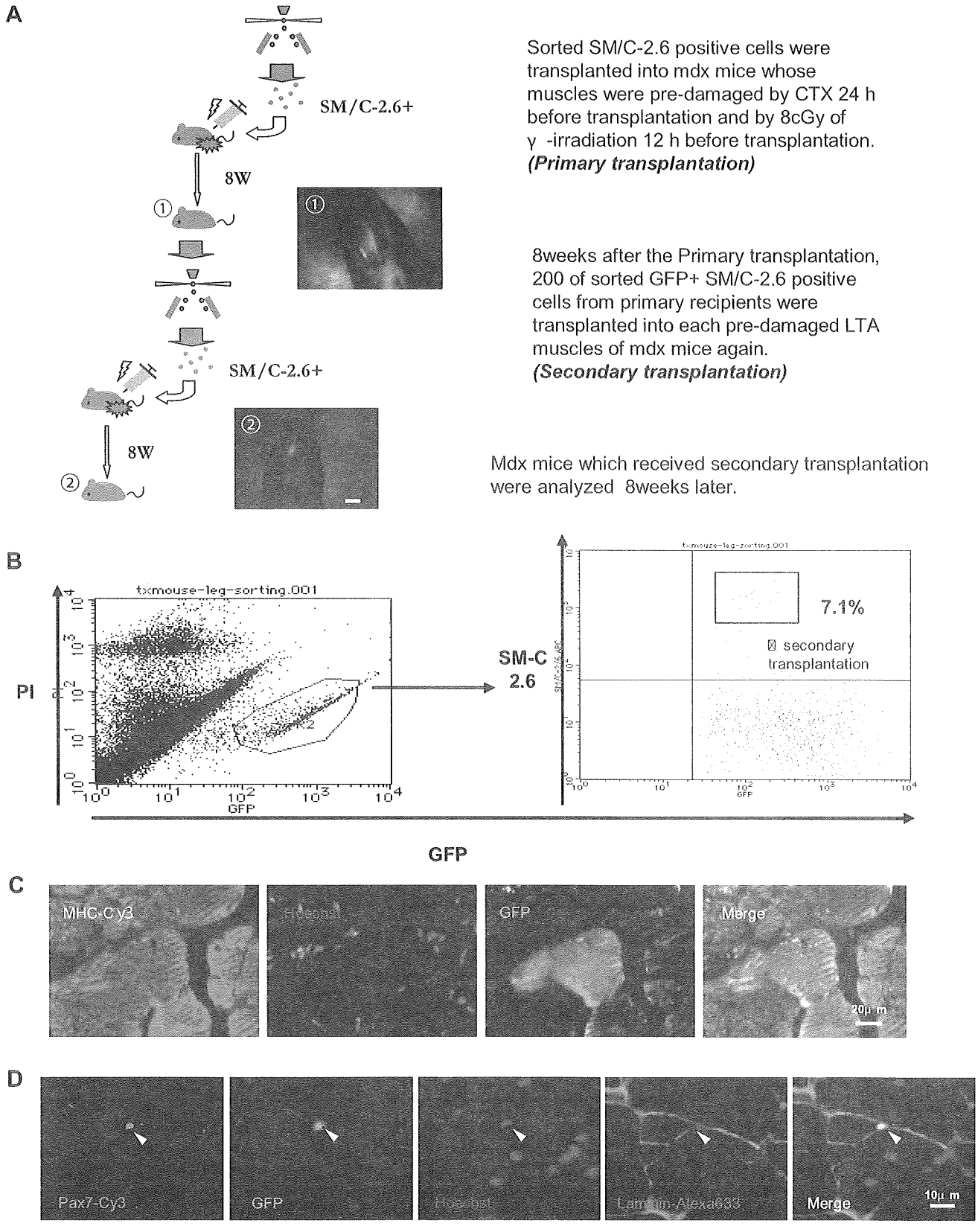

Figure 6. ES-derived satellite-like cells can be secondarily transplanted. *A*) SM/C-2.6-positive cells (2.5×10^4) were transplanted into the LTA muscle of recipient mice in primary transplantation, and as few as 200 SM/C-2.6-positive cells collected from the primary recipients were retransplanted (secondary transplantation) into the LTA muscle of secondary recipient mice. *B*) FACS data of primary transplantation indicated that 7.1% of engrafted (GFP-positive) cells were SM/C-2.6-positive. *C*) Eight weeks after secondary transplantation, immunostaining of LTA muscle for MHC showed that engrafted ES-derived GFP-positive tissues formed mature skeletal muscle fibers. *D*) GFP/Pax7-double-positive cells (arrowhead) located beneath the basal lamina were observed within GFP-positive LTA muscle of secondary recipient mice. Scale bars = 2 mm (*A*); 20 μm (*C*); 10 μm (*D*).

found in recipient mice transplanted with SM/C-2.6-positive cells. Thus, ES-derived satellite-like cells effectively engrafted and provided long-term stem cells, which played an important role in maintenance of the integrity of the surrounding muscle tissue.

ES-derived satellite-like cells can be secondarily transplanted

For a more thorough characterization of the ES-derived satellite-like cells, we performed serial transplantations. Eight weeks after the primary cell transplantation with 2×10^4 SM/C-2.6-positive cells, the LTA muscles of the primary recipient mice were dissected to isolate the engrafted ES-derived cells, 2765 ± 685.9 (n=2; **Fig. 6*A***). The GFP^+/SM/C-2.6-positive cells within the engrafted cells were sorted by FACS (204±33.9; n=2), and only 200 GFP+/SM/C-2.6-positive cells/mouse were transplanted into predamaged LTA muscles of mdx mice (Fig. 6*B*). Eight weeks later (16 wk after the primary transplantation), the recipient mice were analyzed. GFP-positive tissue in the LTA muscle of the secondary recipient mice was observed (Fig. 6*A*). The GFP-positive tissues were confirmed to be MHC-positive mature skeletal muscle (Fig. 6*C*), and surrounding these engrafted GFP-positive skeletal muscle fascicles, dystrophin was observed (Supplemental Fig. 11). GFP/Pax7-double-positive cells located beneath the basal lamina were also detected in the engrafted tissue (Fig. 6*D*). Thus, with only 200 GFP^+SMC/2.6-positive cells, injured skeletal muscle and Pax7+ cells were successfully restored in the secondary recipients. These findings demonstrate that stem cell fraction contained within SM/C-2.6-positive cells was enriched *in vivo* through transplantation.

DISCUSSION

Many attempts have been made to induce mES cells into the skeletal muscle lineage, with hanging drop cultures for EB formation being the most widely applied method (25). However, although EBs contain cells derived from all 3 germ layers, effective induction of mES cells into the myogenic lineage, including myogenic stem cells (satellite cells), has not yet been achieved. Because of the lack of adequate surface markers, purifying ES-derived myogenic precursor/stem cells from differentiated mES cells *in vitro* has been difficult. To overcome these problems, we modified the classic EB culture system by combining it with aspects of the single-fiber culture method. Single-fiber culture (33) has been used for functional evaluation of satellite cells. When a single myofiber is plated on a Matrigel-coated plate with DMEM containing HS, satellite cells migrate out of the fiber and differentiate into myoblasts to form myofibers *in vitro*. Matrigel allows the migrating satellite cells to proliferate before differentiating and fusing into large multinucleated myotubes (35). We hypothesized that this Matrigel environment might be suitable for ES cell differentiation into satellite cells and myoblasts. Therefore, we introduced Matrigel and HS into the classic EB culture system and established an efficient induction system for myogenic lineage cells, including cells expressing Pax7, a commonly recognized marker for skeletal muscle stem cells. Furthermore, we also successfully enriched ES-derived Pax7-positive myogenic precursor/stem cells using the SM/C-2.6 antibody.

The steps in ES cell induction are thought to be homologous to normal embryogenesis. During normal skeletal myogenesis, the initial wave of myogenic precursor cells in the dermomyotome express Myf5/MRF4 and Pax3, followed by a wave of Pax3/Pax7 expression (36). These waves of myogenesis act upstream of the primary myogenic transcription factor MyoD (37-39). In myotome formation skeletal myogenesis begins with myoblasts, termed somitic myoblasts, which appear at approximately E8.5, followed by the appearance of embryonic myoblasts (E11.5), fetal myoblasts (E16.5), and, ultimately, satellite cells, which are responsible for postnatal muscle regeneration (40). Our RT-PCR results (Fig. 1*J*) showed an earlier appearance of Pax3 expression, on d 3 + 3, followed by Pax3/Pax7 expression on d 3 + 3 + 7 and stronger expression of Pax3 than Pax7. These results resemble normal myogenesis, in which the primary wave of myogenesis is followed by a secondary wave of Pax3/Pax7-dependent myogenesis (41). Considering that in the time course of myogenesis satellite cells emerge during late fetal development, ES-derived Pax7-positive cells were collected on d 3 + 3 + 14 in an attempt to acquire cells that correspond to those of the late fetal to neonatal period. However, RT-PCR results of myogenic factors in SM/C-2.6-positive cells (Fig. 2*B*) indicated that these ES-derived SM/C-2.6-positive cells are a heterogeneous population, because they express not only Pax3 and Pax7 but also Myf5 and c-met. Although further confirmation is needed, we hypothesize that both embryonic/fetal myoblasts expressing Myf-5 and/or c-met and satellite/long-term stem cells expressing Pax3/Pax7 are present.

To confirm that the ES-derived SM/C-2.6-positive cell population contained functional satellite cells, the muscle regeneration and self-renewal capacities were examined. Recently Collins *et al.* established an excellent system in which sequential damage to the muscle of a recipient mouse was applied, to evaluate both muscle regeneration and self-renewal (14) Using their experimental approach, a significant increase in numbers of both ES-derived GFP-positive muscle fascicles and GFP/Pax7-double-positive cells was observed in mice that received a second injury. This result not only demonstrates the myogenic ability of ES-derived cells but also strongly supports the idea that these cells undergo self-renewal *in vivo*.

Analysis of long-term engraftment is an important method to verify self-renewal ability, for 2 reasons. First, ES-derived satellite cells must be able to engraft for long periods of time in order to provide the amount of progeny needed for repairing damaged tissue for an

extended period. In our study the ES-derived GFP-positive skeletal muscle tissues and Pax7-positive cells engrafted up to 24 wk and were located beneath the basal lamina, which is consistent with the anatomical definition of satellite cells. Although the number of GFP-positive fascicles at 24 wk decreased compared to 12 wk, this diminution may be due to the heterogeneity of ES-derived SM/C-2.6-positive cells as we mentioned. Because myoblasts cannot support myogenesis in the long term, we believe that GFP-positive fascicles at 24 wk are products of ES-derived satellite-like cells. Second, one of the potential risks of ES cell transplantation is teratoma formation. Considering clinical applications, it is extremely important to prevent formation of teratomas in the recipients. In our study more than 60 transplanted mice were evaluated through gross morphological and histological examination. There were no teratomas formed in mice that received SM/C-2.6-positive cells, and only 1 teratoma was found among the mice that received SM/C-2.6-negative cells. This result suggests that the risk of tumor formation by the ES cells was eliminated by using sorted SM/C-2.6-positive cells.

In addition to the sequential damage model and the long-term engraftment evaluation, we performed serial transplantations to further confirm the stem cell properties of these ES-derived SM/C-2.6-positive cells. Serial transplantation enables the identification and separation of long-term stem cells from short-term progenitors (42). To eliminate myoblast involvement, we designed a serial transplantation protocol of 8 + 8 wk (*i.e.*, a second transplantation 8 wk after the primary transplantation and an analysis of recipient mice 8 wk after the second transplantation). Strikingly these recollected ES-derived SM/C-2.6-positive cells showed significantly higher engraftment efficiency compared to the primary transplantation. In the previous reports engraftment efficiencies of myoblasts transplantation was ~0.1-0.2%, with the highest reported value being 2% (43-45). This engraftment efficiency is similar to our primary transplantation (0.2-0.8%) as well as the plating efficiency of SM/C-2.6-positive cells *in vitro* (0.07%). In our study as few as 200 recollected ES-derived SM/C-2.6-positive cells were transplanted in the second transplantation, and 29.0 ± 0.47 (n=2) fascicles were observed, which indicates 14.7% of higher engraftment efficiency. Thus, through the serial transplantation, ES-derived stem cell fraction was purified. A comparison of these SM/C-2.6-positive cells before and after injection might help to characterize the stem cell fraction derived from ES cells.

There have been few reports describing transplantation of ES-derived myogenic cells into injured muscles, and the report of engraftable skeletal myoblasts derived from human ES cells represents significant progress (26). Recently Darabi *et al.* (46) have reported that by introducing Pax3 into mouse embryoid bodies, autonomous myogenesis was initiated *in vitro,* and Pax3-induced cells regenerated skeletal muscles *in vivo* by sorting the PDGF-a+Flk-1- cells. The Pax3 expression was not observed until 7 d of differentiation culture, but introduced Pax3 expression pushed EBs to myogenic differentiation. Interestingly, we observed Pax3 expression at d 3 + 3 weakly and d 3 + 3 + 7 strongly, and gene expression process in our culture is very similar to theirs. In prolonged culture using Matrigel and HS, EBs were able to initiate myogenesis without gene modification in our system.

In conclusion, we successfully generated transplantable myogenic cells, including satellite-like cells, from mES cells. The ES-derived myogenic precursor/stem cells could be enriched using a novel antibody, SM/C-2.6. These ES-derived SM/C-2.6-positive cells possess a high myogenic potential, participate in muscle regeneration, and are located beneath the basal lamina where satellite cells normally reside. The self-renewal of these ES-derived satellite-like cells enabled them to survive long-term engraftment, up to 24 wk. Through serial transplantation, these ES-derived SM/C-2.6-positive cells were further enriched and produced a high engraftment efficiency of 14.7%.

Our success in inducing mES cells to form functional muscle stem cells, the satellite-like cells, will provide an important foundation for clinical applications in the treatment of DMD patients. FJ

This work was supported by a Grant-in-Aid for Scientific Research (S) (19109006) and a Grant-in-Aid for Scientific Research (B) (18390298) from the Ministry of Education, Science, Technology, Sports, and Culture of Japan.

REFERENCES

1. Nawrotzki, R., Blake, D. J., and Davies, K. E. (1996) The genetic basis of neuromuscular disorders. *Trends Genet.* **12,** 294–298
2. Emery, A. E. (2002) The muscular dystrophies. *Lancet* **359,** 687–695
3. Michalak, M., and Opas, M. (1997) Functions of dystrophin and dystrophin associated proteins. *Curr. Opin. Neurol.* **10,** 436–442
4. Suzuki, A., Yoshida, M., Hayashi, K., Mizuno, Y., Hagiwara, Y., and Ozawa, E. (1994) Molecular organization at the glycoprotein-complex-binding site of dystrophin. Three dystrophin-associated proteins bind directly to the carboxy-terminal portion of dystrophin. *Eur. J. Biochem./FEBS* **220,** 283–292
5. Bonilla, E., Samitt, C. E., Miranda, A. F., Hays, A. P., Salviati, G., DiMauro, S., Kunkel, L. M., Hoffman, E. P., and Rowland, L. P. (1988) Duchenne muscular dystrophy: deficiency of dystrophin at the muscle cell surface. *Cell* **54,** 447–452
6. Mauro, A. (1961) Satellite cell of skeletal muscle fibers. *J. Biophys. Biochem. Cytol.* **9,** 493–495
7. Moss, F. P., and Leblond, C. P. (1971) Satellite cells as the source of nuclei in muscles of growing rats. *Anat. Rec.* **170,** 421–435
8. Snow, M. H. (1978) An autoradiographic study of satellite cell differentiation into regenerating myotubes following transplantation of muscles in young rats. *Cell Tissue Res.* **186,** 535–540
9. Jejurikar, S. S., and Kuzon, W. M., Jr. (2003) Satellite cell depletion in degenerative skeletal muscle. *Apoptosis* **8,** 573–578
10. Schultz, E., and Jaryszak, D. L. (1985) Effects of skeletal muscle regeneration on the proliferation potential of satellite cells. *Mech. Ageing Dev.* **30,** 63–72
11. Webster, C., and Blau, H. M. (1990) Accelerated age-related decline in replicative life-span of Duchenne muscular dystrophy myoblasts: implications for cell and gene therapy. *Somat. Cell Mol. Genet.* **16,** 557–565
12. Hashimoto, N., Murase, T., Kondo, S., Okuda, A., and Inagawa-Ogashiwa, M. (2004) Muscle reconstitution by muscle satellite

cell descendants with stem cell-like properties. *Development (Camb.)* **131,** 5481–5490
13. Montarras, D., Morgan, J., Collins, C., Relaix, F., Zaffran, S., Cumano, A., Partridge, T., and Buckingham, M. (2005) Direct isolation of satellite cells for skeletal muscle regeneration. *Science* **309,** 2064–2067
14. Collins, C. A., Olsen, I., Zammit, P. S., Heslop, L., Petrie, A., Partridge, T. A., and Morgan, J. E. (2005) Stem cell function, self-renewal, and behavioral heterogeneity of cells from the adult muscle satellite cell niche. *Cell* **122,** 289–301
15. Partridge, T. A., Morgan, J. E., Coulton, G. R., Hoffman, E. P., and Kunkel, L. M. (1989) Conversion of mdx myofibres from dystrophin-negative to -positive by injection of normal myoblasts. *Nature* **337,** 176–179
16. Mendell, J. R., Kissel, J. T., Amato, A. A., King, W., Signore, L., Prior, T. W., Sahenk, Z., Benson, S., McAndrew, P. E., Rice, R., Nagaraja, H., Stephens, R., Lantry, L., Morris, G. E., and Burghes, A. H. M. (1995) Myoblast transfer in the treatment of Duchenne's muscular dystrophy. *N. Engl. J. Med.* **333,** 832–838
17. Weissman, I. L., Anderson, D. J., and Gage, F. (2001) Stem and progenitor cells: origins, phenotypes, lineage commitments, and transdifferentiations. *Annu. Rev. Cell Dev. Biol.* **17,** 387–403
18. Relaix, F., Montarras, D., Zaffran, S., Gayraud-Morel, B., Rocancourt, D., Tajbakhsh, S., Mansouri, A., Cumano, A., and Buckingham, M. (2006) Pax3 and Pax7 have distinct and overlapping functions in adult muscle progenitor cells. *J. Cell Biol.* **172,** 91–102
19. Seale, P., Sabourin, L. A., Girgis-Gabardo, A., Mansouri, A., Gruss, P., and Rudnicki, M. A. (2000) Pax7 is required for the specification of myogenic satellite cells. *Cell* **102,** 777–786
20. Cornelison, D. D., and Wold, B. J. (1997) Single-cell analysis of regulatory gene expression in quiescent and activated mouse skeletal muscle satellite cells. *Dev. Biol.* **191,** 270–283
21. Hollnagel, A., Grund, C., Franke, W. W., and Arnold, H. H. (2002) The cell adhesion molecule M-cadherin is not essential for muscle development and regeneration. *Mol. Cell. Biol.* **22,** 4760–4770
22. Bottaro, D. P., Rubin, J. S., Faletto, D. L., Chan, A. M., Kmiecik, T. E., Vande Woude, G. F., and Aaronson, S. A. (1991) Identification of the hepatocyte growth factor receptor as the c-met proto-oncogene product. *Science* **251,** 802–804
23. Fukada, S., Higuchi, S., Segawa, M., Koda, K., Yamamoto, Y., Tsujikawa, K., Kohama, Y., Uezumi, A., Imamura, M., Miyagoe-Suzuki, Y., Takeda, S., and Yamamoto, H. (2004) Purification and cell-surface marker characterization of quiescent satellite cells from murine skeletal muscle by a novel monoclonal antibody. *Exp. Cell Res.* **296,** 245–255
24. Dekel, I., Magal, Y., Pearson-White, S., Emerson, C. P., and Shani, M. (1992) Conditional conversion of ES cells to skeletal muscle by an exogenous MyoD1 gene. *New Biol.* **4,** 217–224
25. Rohwedel, J., Maltsev, V., Bober, E., Arnold, H. H., Hescheler, J., and Wobus, A. M. (1994) Muscle cell differentiation of embryonic stem cells reflects myogenesis in vivo: developmentally regulated expression of myogenic determination genes and functional expression of ionic currents. *Dev. Biol.* **164,** 87–101
26. Barberi, T., Bradbury, M., Dincer, Z., Panagiotakos, G., Socci, N. D., and Studer, L. (2007) Derivation of engraftable skeletal myoblasts from human embryonic stem cells. *Nat. Med.* **13,** 642–648
27. Doetschman, T. C., Eistetter, H., Katz, M., Schmidt, W., and Kemler, R. (1985) The in vitro development of blastocyst-derived embryonic stem cell lines: formation of visceral yolk sac, blood islands and myocardium. *J. Embryol. Exp. Morphol.* **87,** 27–45
28. Niwa, H., Yamamura, K., and Miyazaki, J. (1991) Efficient selection for high-expression transfectants with a novel eukaryotic vector. *Gene* **108,** 193–199
29. Yoshimoto, M., Chang, H., Shiota, M., Kobayashi, H., Umeda, K., Kawakami, A., Heike, T., and Nakahata, T. (2005) Two different roles of purified CD45+c-Kit+Sca-1+Lin-cells after transplantation in muscles. *Stem Cells (Dayton)* **23,** 610–618
30. Harris, J. B. (2003) Myotoxic phospholipases A2 and the regeneration of skeletal muscles. *Toxicon* **42,** 933–945
31. Fukada, S., Miyagoe-Suzuki, Y., Tsukihara, H., Yuasa, K., Higuchi, S., Ono, S., Tsujikawa, K., Takeda, S., and Yamamoto, H. (2002) Muscle regeneration by reconstitution with bone marrow or fetal liver cells from green fluorescent protein-gene transgenic mice. *J. Cell Sci.* **115,** 1285–1293
32. Gross, J. G., and Morgan, J. E. (1999) Muscle precursor cells injected into irradiated mdx mouse muscle persist after serial injury. *Muscle Nerve* **22,** 174–185
33. Rosenblatt, J. D., Lunt, A. I., Parry, D. J., and Partridge, T. A. (1995) Culturing satellite cells from living single muscle fiber explants. *In Vitro Cell. Dev. Biol.* **31,** 773–779
34. Dhawan, J., and Rando, T. A. (2005) Stem cells in postnatal myogenesis: molecular mechanisms of satellite cell quiescence, activation and replenishment. *Trends Cell Biol.* **15,** 666–673
35. Zammit, P. S., Relaix, F., Nagata, Y., Ruiz, A. P., Collins, C. A., Partridge, T. A., and Beauchamp, J. R. (2006) Pax7 and myogenic progression in skeletal muscle satellite cells. *J. Cell Sci.* **119,** 1824–1832
36. Relaix, F., Rocancourt, D., Mansouri, A., and Buckingham, M. (2005) A Pax3/Pax7-dependent population of skeletal muscle progenitor cells. *Nature* **435,** 948–953
37. Tajbakhsh, S., Rocancourt, D., Cossu, G., and Buckingham, M. (1997) Redefining the genetic hierarchies controlling skeletal myogenesis: Pax-3 and Myf-5 act upstream of MyoD. *Cell* **89,** 127–138
38. Kiefer, J. C., and Hauschka, S. D. (2001) Myf-5 is transiently expressed in nonmuscle mesoderm and exhibits dynamic regional changes within the presegmented mesoderm and somites I-IV. *Dev. Biol.* **232,** 77–90
39. Hirsinger, E., Malapert, P., Dubrulle, J., Delfini, M. C., Duprez, D., Henrique, D., Ish-Horowicz, D., and Pourquie, O. (2001) Notch signalling acts in postmitotic avian myogenic cells to control MyoD activation. *Development (Camb.)* **128,** 107–116
40. Smith, T. H., Block, N. E., Rhodes, S. J., Konieczny, S. F., and Miller, J. B. (1993) A unique pattern of expression of the four muscle regulatory factor proteins distinguishes somitic from embryonic, fetal and newborn mouse myogenic cells. *Development (Camb.)* **117,** 1125–1133
41. Kassar-Duchossoy, L., Giacone, E., Gayraud-Morel, B., Jory, A., Gomes, D., and Tajbakhsh, S. (2005) Pax3/Pax7 mark a novel population of primitive myogenic cells during development. *Genes Dev.* **19,** 1426–1431
42. Harrison, D. E., Astle, C. M., and Delaittre, J. A. (1978) Loss of proliferative capacity in immunohemopoietic stem cells caused by serial transplantation rather than aging. *J. Exp. Med.* **147,** 1526–1531
43. Yao, S. N., and Kurachi, K. (1993) Implanted myoblasts not only fuse with myofibers but also survive as muscle precursor cells. *J. Cell Sci.* **105**(Pt. 4), 957–963
44. Rando, T. A., and Blau, H. M. (1994) Primary mouse myoblast purification, characterization, and transplantation for cell-mediated gene therapy. *J. Cell Biol.* **125,** 1275–1287
45. Sherwood, R. I., Christensen, J. L., Conboy, I. M., Conboy, M. J., Rando, T. A., Weissman, I. L., and Wagers, A. J. (2004) Isolation of adult mouse myogenic progenitors: functional heterogeneity of cells within and engrafting skeletal muscle. *Cell* **119,** 543–554
46. Darabi, R., Gehlbach, K., Bachoo, R. M., Kamath, S., Osawa, M., Kamm, K. E., Kyba, M., and Perlingeiro, R. C. (2008) Functional skeletal muscle regeneration from differentiating embryonic stem cells. *Nat. Med.* **14,** 134–143

Received for publication October 21, 2008.
Accepted for publication January 8, 2009.

Biochemical and Biophysical Research Communications 387 (2009) 482–488

Contents lists available at ScienceDirect

Biochemical and Biophysical Research Communications

journal homepage: www.elsevier.com/locate/ybbrc

The effects of cardioactive drugs on cardiomyocytes derived from human induced pluripotent stem cells

Noritaka Yokoo [a], Shiro Baba [a], Shinji Kaichi [a], Akira Niwa [a], Takahiro Mima [a], Hiraku Doi [a], Shinya Yamanaka [b], Tatsutoshi Nakahata [b], Toshio Heike [a,*]

[a] Department of Pediatrics, Graduate School of Medicine, Kyoto University, 54 Kawahara-cho, Shogoin, Sakyo-ku, Kyoto 606-8507, Japan
[b] Center for iPS Cell Research and Application (CiRA), Institute for Integrated Cell-Material Sciences, Kyoto University, 53 Kawahara-cho, Shogoin, Sakyo-ku, Kyoto 606-8507, Japan

ARTICLE INFO

Article history:
Received 7 July 2009
Available online 16 July 2009

Keywords:
Human induced pluripotent stem cell
Human embryonic stem cell
Cardiomyocytes
Drug loading test
Arrhythmia

ABSTRACT

Developing effective drug therapies for arrhythmic diseases is hampered by the fact that the same drug can work well in some individuals but not in others. Human induced pluripotent stem (iPS) cells have been vetted as useful tools for drug screening. However, cardioactive drugs have not been shown to have the same effects on iPS cell-derived human cardiomyocytes as on embryonic stem (ES) cell-derived cardiomyocytes or human cardiomyocytes in a clinical setting. Here we show that current cardioactive drugs affect the beating frequency and contractility of iPS cell-derived cardiomyocytes in much the same way as they do ES cell-derived cardiomyocytes, and the results were compatible with empirical results in the clinic. Thus, human iPS cells could become an attractive tool to investigate the effects of cardioactive drugs at the individual level and to screen for individually tailored drugs against cardiac arrhythmic diseases.

Introduction

The long-QT syndrome (LQTS) is characterized by an abnormal prolongation of the QT-interval on the ECG and an increased risk of sudden death, due to ventricular fibrillation known as Torsade de Pointes (TdP) [1]. In a previous study [2], four patients died suddenly (1.3% per year) during an average follow-up period of 26 months per patient and among 196 idiopathic LQTS patients, 27 experienced one or more syncopal episodes (8.6% per year). Molecular genetic studies have revealed several forms of congenital LQTS caused by mutations in genes coding for potassium, sodium and calcium channels or membrane adapters [3–6]. Preliminary clinical studies have since suggested the feasibility of performing genotype-specific therapy with therapeutic agents that abbreviate the QT-interval [7]. But it is difficult to select the correct drug because within the same LQTS subtype, the same drug can sometimes have different effects depending on the patient.

Furthermore, the diagnosis of LQTS subtypes is difficult. Genetic testing can only identify 50–75% of probands [8]. So an epinephrine challenge is needed in some patients to diagnose LQTS in a clinical setting [9]. However, this test sometimes induces TdP, so it must be done under careful patient surveillance.

The generation of iPS cells from human fibroblast using a combination of 4 transcription factors (*Oct3/4*, *Sox2*, *Klf4*, and *c-Myc*) has opened remarkable new avenues for not only basic research but also regenerative medicine, understanding of disease mechanisms, drug screening, and toxicology [10]. A recent study reported the generation of disease-specific iPS cell lines from patients with a variety of diseases [11]. If patient-specific iPS cells could be commonly generated and employed in a clinical setting, they could become a useful tool for selecting the best drug for individual LQTS patients.

But there has been no report that cardiomyocytes derived from human iPS cells respond to drugs in the same way as human cardiomyocytes. It is important to investigate whether cardiomyocytes derived from human iPS cells react to drugs in the same way as human cardiomyocytes, if patient-specific iPS cells are to be used in a clinical setting for drug screening. Previous studies have hinted that some drugs produce the same effects in cardiomyocytes as in cardiomyocytes derived from ES cells [12–14]. In this study, we investigated whether cardiomyocytes derived human iPS cells responded to drugs in the same way as in cardiomyocytes derived from human ES cells with respect to beating frequency and contractility, and we compared these results with previously described clinical empirical results [15].

Materials and methods

Human iPS and human ES cell culture. We used human ES cell line, KhES1, and human iPS cell lines 201B7. Human iPS cells and human ES cells were maintained on mitomycin-C (Kyowa Hakkoh)

* Corresponding author. Fax: +81 75 752 2361.
E-mail address: heike@kuhp.kyoto-u.ac.jp (T. Heike).

0006-291X/$ - see front matter © 2009 Elsevier Inc. All rights reserved.
doi:10.1016/j.bbrc.2009.07.052

treated mouse embryonic fibroblasts (MEFs) or SNLs on cell culture dishes. In brief, both human iPS and human ES cells were maintained in DMEM/F12 culture medium (SIGMA) supplemented with 20% knock-out serum replacement (Gibco), 0.1 mmol/L nonessential amino acids (Gibco), 4 mmol/L L-glutamine, 0.8 μmol/L basic fibroblast growth factor (bFGF) (Invitrogen).

Embryoid body formation and cardiac differentiation. Colonies were detached from cell culture dishes by incubating them with PBS containing 0.25% trypsin (Gibco) and 1 mg/mL collagenase I (Worthington) at 37 °C for 3–4 min. The cells were then placed in petri dishes (Sterilin) in suspension cultures for 7 days with maintenance medium supplemented with 5 ng/ml bFGF. Embryoid bodies (EBs) were then plated on 0.1% gelatin-coated 6-well culture plates (BD Biosciences) and cultured in cardiac differentiation medium, consisting of alpha MEM (Gibco) supplemented with 0.5 μmol/L 2ME and 10% FCS (Hyclone) (changed once every 7 days). Contractile colonies appeared 15–25 days after plating on gelatin-coated dishes (Fig. 1A).

Reverse transcriptase polymerase chain reaction (RT-PCR). Total RNA was isolated using TRIzol Reagent (Invitrogen) from undifferentiated iPS cells, EBs derived from human iPS cells, the contracting areas of differentiated human iPS cells, and human right ventricular tissue (obtained by a tetralogy of Fallot patient that had received a right flow ventricular tract ventriculotomy). Total RNA was used for oligo (dT) 12–18-primed reverse transcription using the Super Script II First-Strand Synthesis System (Invitrogen). RT-PCR was carried out using Ex Taq (TAKARA BIO). PCR conditions included denaturation at 94 °C for 30 s, annealing at 60 °C for 30 s, and extension at 55–65 °C for 1 min for 25–35 cycles, with a final extension at 72 °C for 7 min. Primers used are listed in Table 3.

Immunohistochemistry. Contractile colonies were partitioned into small particles using collagenase I (Worthington) for 2 h at 37 °C. The cells were then washed and plated on 6-well culture plates coated with 0.1% gelatin for 2 or 3 days to allow attachment. Cells were fixed in 4% paraformaldehyde for 15 min at 4 °C. Then the cells were incubated with primary antibodies, such as polyclonal anti-cardiac Troponin I (IgG, 1:50 dilution; Santa Cruz Biotechnology), polyclonal anti-MLC2v (IgG, 1:50 dilution; Santa Cruz Biotechnology), or polyclonal anti-ANP (IgG, 1:250 dilution; Chemicon) in 2% skim milk with 0.1% Triton X-100 overnight at 4 °C. Secondary antibodies were cyanine 3 (Cy3)-conjugated donkey anti-rat IgG (1:200 dilution; Jackson Immunoresearch), Cy3-conjugated donkey anti-rabbit IgG (1:200 dilution; Jackson Immunoresearch), and Cy3-conjugated donkey anti-goat IgG (1:200 dilution; Jackson Immunoresearch). Nuclei were counter-stained with Hoechst 33342 (Molecular probes).

Electrophysiological examination. Microelectrode arrays analysis was performed to investigate the electrophysiological potential of cardiomyocytes derived from human iPS cells using the MED 64 system (Alpha MED Sciences) [16–18]. Micro-dissected contracting areas were plated on MED-probe dishes (Alpha MED Sciences) followed by incubation for 3–7 days to allow attachment. The potentials of the contractile colonies derived from these cells were then recorded.

Drug loading test. Differentiation medium was replaced with alpha MEM containing 10 mmol/L HEPES buffer (Nacalai tesque), 7 mol/L NaCl, and 0.5 μmol/L 2ME, which was adjusted to pH 7.4 with NaOH. After 10 min incubation at 37 °C, the frequency and contractility of the contractile colonies were measured in a movie recorded by a VB 7000 (KEYENCE) camera under drug-free medium conditions as well as under drug conditions with three different drug concentrations. Beating colonies were selected when the beating rate was 40/min to 60/min under drug-free medium conditions. Colonies whose contractile motion was distended were excluded. Loading drugs were as follows; isoproterenol (SIGMA), adrenaline (Dai-ichi Sankyo), propranolol (SIGMA), procainamide (Dai-ichi Sankyo), mexiletine (Boehringer Ingelheim), flecainide (Eisai), verapamil (SIGMA), and amiodarone (Sanofi-aventis).

Analysis of beating rate and contractility. Beating rates were counted based on the video recordings. Recently, some papers reported that video-edge detecting systems are useful for calculating the contractility of contractile colonies [12]. We imitated this method and calculated the contractility of colonies. In brief, we extracted the still images of systolic phase and diastolic phase from the recorded video images. The major axis of each phase was measured and the contractile index was defined as $a - b/a$ (a: length of diastolic phase, b: the length of systolic phase) (Fig. 4A).

Statistics. Data are presented as means ± SEM. Statistical significance was determined by the unpaired t-test for two samples and one-way ANOVA followed by the Scheffe test for more than three samples. P values <0.05 were considered to be statistically significant.

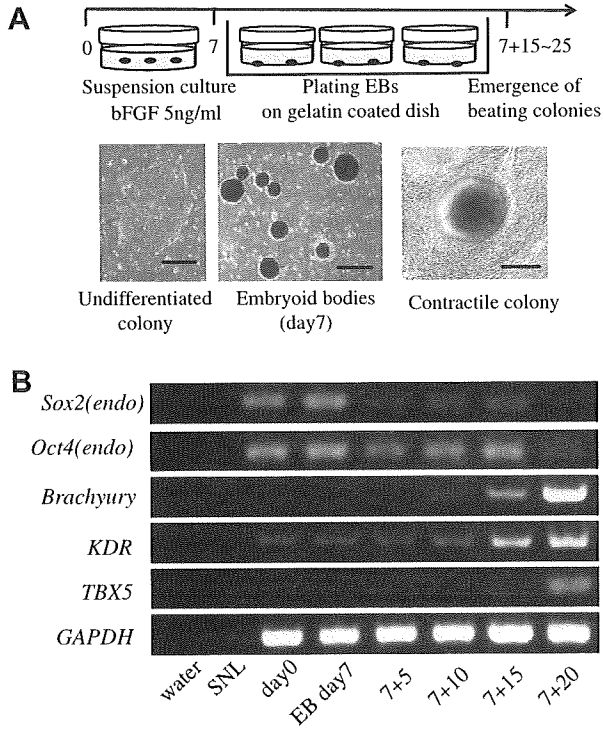

Fig. 1. An outline of the protocol used for the differentiation of human iPS cells and human ES cells. Scale bars = 200 μm (A). Time course analysis of immature gene expression, mesodermal markers, and cardiac progenitor markers during differentiation (B).

Results

Time course analysis of gene expression during cardiac differentiation

First, we examined the time course of gene expression during cardiac differentiation of human iPS cells by RT-PCR to compare it with that of normal embryogenesis (Fig. 1B). Undifferentiated human iPS cells strongly expressed endogenous *Oct4* and *Sox2*, which are undifferentiated cell markers, but did not express the mesodermal marker *Brachyury* or the cardiac progenitor marker *TBX5* (Fig. 1B). *KDR* was weakly expressed. These results show that undifferentiated human iPS cells have similar properties to undifferentiated human ES cells [19]. Endogenous *Oct4* and *Sox2* expression gradually decreased during culture in differentiation medium. The

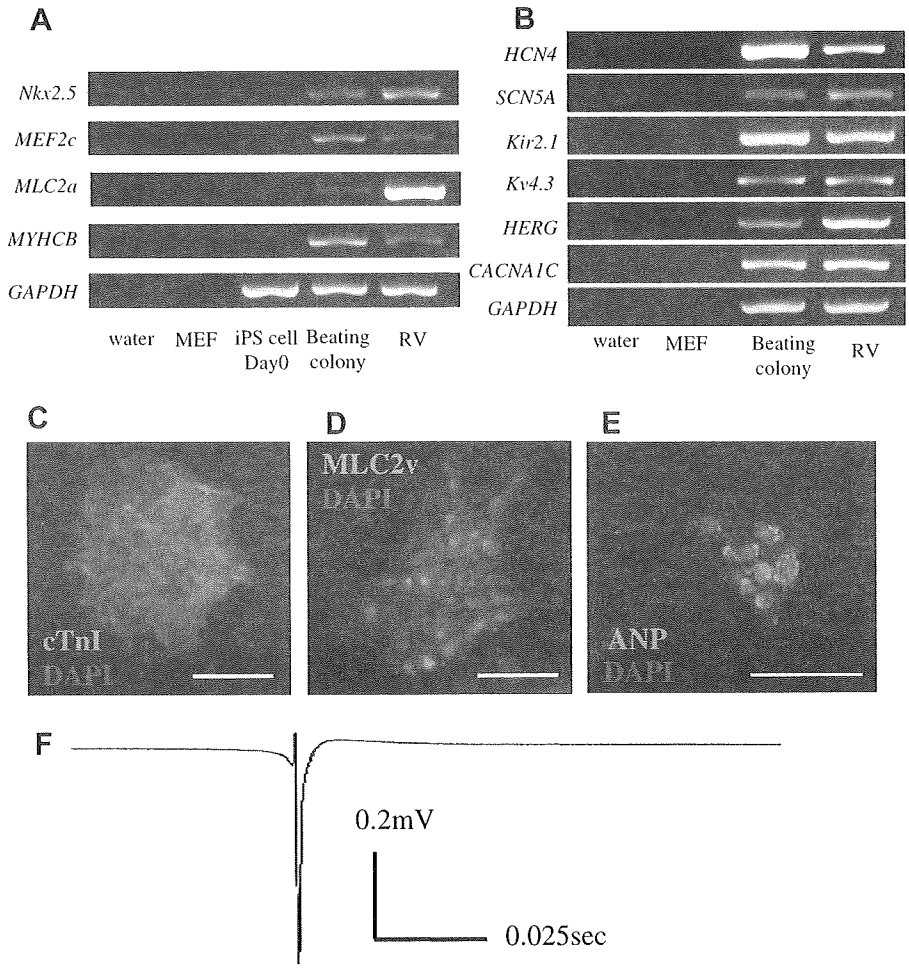

Fig. 2. Gene expression analyses of cardiac markers by RT-PCR (A). Gene expression analysis of ion channel related genes (B). Immunohistochemistry of contractile colonies. Colonies were stained with cTnI (C), MLC2v (D), or ANP (E). Scale bars = 100 μm. Field potentials of contractile colonies measured by the MED 64 system (F).

expression of the mesodermal marker *Brachyury* increased from day 10 after EB formation. The expression of *KDR* also gradually increased from day 10 after EB formation. These patterns of mesodermal marker expression are compatible with those of human ES cells as previously described [19]. The cardiac progenitor marker *TBX5* was expressed from day 20 after EB formation, which is compatible with the gene expression patterns seen during cardiac formation in embryogenesis and human ES cell differentiation as previously described [19]. The result additionally suggests that human iPS cells differentiated into the mesodermal lineage and then differentiated into contractile colonies via cardiac progenitor cells.

Cardiac differentiation of human iPS cells via EBs

Next, we examined the contractile colonies consisting of cardiac-specific cells. Contractile colonies were observed from 15 to 25 days after EB formation both in human iPS and human ES cell populations. This result demonstrates that our differentiation methods could generate contractile colonies from both human iPS cells and human ES cells. Next, we investigated whether these contractile colonies were human cardiomyocytes. For this purpose, we carried out RT-PCR and examined for the expression of cardiac cell markers. RT-PCR showed that contractile colonies expressed cardiac markers *Nkx2.5*, *MEF2c*, *MLC2a*, and *MYHCB* (Fig. 2A). Moreover, we carried out immunohistochemical analysis to confirm that the contractile colonies were human cardiomyocytes. Contractile colonies were stained by the cardiac cell marker, cTnI, the ventricular cell marker, MLC2v, and the atrial cell marker, ANP. The colonies were also stained by cTnI, and some of them were stained by MLC2v or ANP (Fig. 2C–E). These results of immunohistochemical analysis confirmed that the contractile colonies were indeed human cardiomyocytes.

Electrical analysis of contractile colonies

To investigate whether the contractile colonies that expressed cardiac markers were electrically functional cardiac colonies, we measured their electrical potentials by microelectrode array analysis using the MED 64 system (Alpha MED Sciences) [16–18]. The field potentials of the contractile colonies were comparable to those of cardiomyocytes derived from human ES cells as previously reported (Fig. 2F) [16–18]. Moreover, RT-PCR showed that these cells expressed the If channel (*HCN4*), the L-type calcium channel (*CACNA1C*), the sodium channel (*SCN5A*), the inward rectifier (*Kir2.1*), the transient outward channel (*Kv4.3*), and the delayed rectifier IKr (*HERG*) (Fig. 2B).

Effects of drugs on the beating frequency of cardiomyocytes derived from human iPS cells

We next investigated whether the cardiomyocytes derived from iPS cells reacted with cardioactive drugs in the same manner as

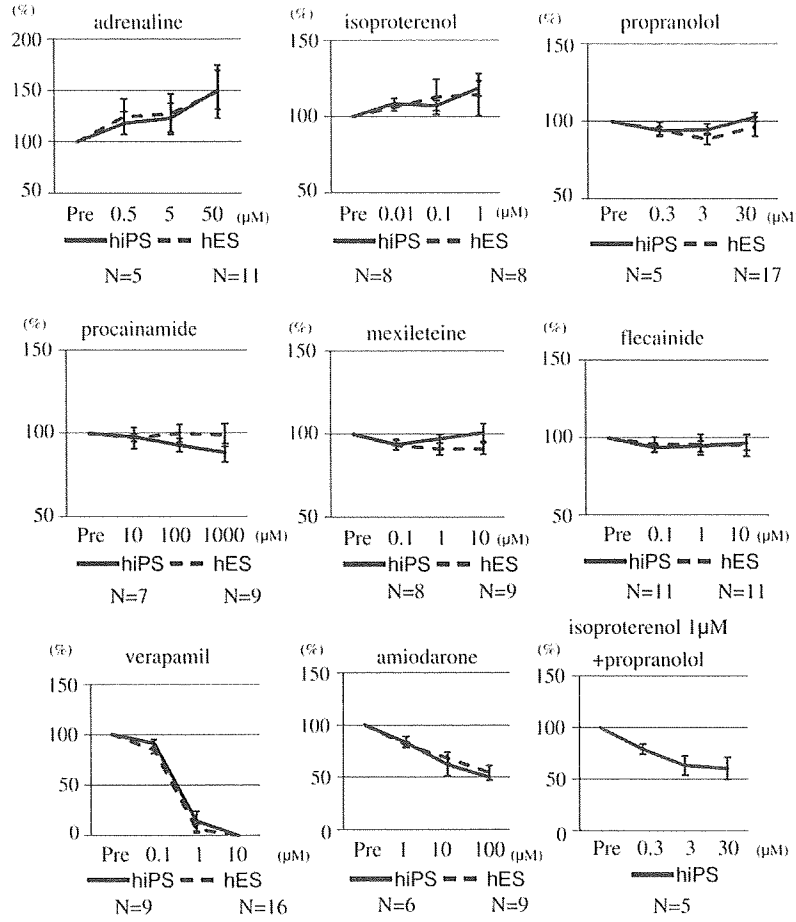

Fig. 3. The effects of cardioactive drugs on the beating rates of contractile colonies derived from human iPS cells and human ES cells. Adrenaline, isoproterenol, verapamil, amiodarone, and isoproterenol + propranolol had statistically significant effects between pre-drug loading and the maximum concentration of the drug used in cardiomyocytes derived from human iPS cells ($P < 0.05$). There were no statistically significant differences between the concentrations of drugs that elicited effects in human iPS cells and those that elicited effects in human ES cells.

cardiomyocytes derived from human ES cells by performing drug loading tests. First we compared the beating frequencies of these two cell populations. A total of eight drugs were tested (see Table 1 for the list of drugs and their concentrations). The β stimulants, adrenaline and isoproterenol increased beating frequency in a dose dependent manner. The β blocker, propranolol, and the Na channel blockers, procainamide, mexiletine, and flecainide had no effect on beating frequency. The Ca channel blocker verapamil decreased beating frequency in a dose dependent manner, and all contractile colonies ceased to contract when 1×10^{-5} M verapamil was loaded. Amiodarone, which mainly acts as a K channel blocker, decreased beating frequency in a dose dependent manner. We carried out β blocker loading in the presence of 1×10^{-6} M isoproterenol in order to mimic conditions *in vivo* [20]. Under this condition, the beating frequency decreased in a dose dependent manner. There were no statistical differences between the drug concentrations required to elicit the effects in human iPS cells and those required to elicit the effects in cardiomyocytes derived from human ES cells (Fig. 3). Previous reports showed that some drugs had similar effects on the beating frequency of cardiomyocytes derived from ES cells and on *bone-fide* human cardiomyocytes, suggesting that human iPS cells and cardiomyocytes respond similarly to these drugs as well [12–14]. Table 2 shows a comparison of the effects of drug loading on human iPS cells and the effects of these drugs in a clinical setting [15]. As the effects are broadly similar and occur within the same range of drug concentrations, we conclude that cardiomyocytes derived from human iPS cells are a good model for testing the effects of drugs on the beating frequency of human cardiomyocytes. The results are also compatible with previously reported clinical empirical results [15].

The effects of drugs on the contractility of cardiomyocytes derived from human iPS cells

Next, we investigated the effects of drugs on the contractility of human iPS cells and cardiomyocytes derived from human ES cells. The results showed that adrenaline and isoproterenol increased contractility in a dose dependent manner. Propranolol, mexiletine, or amiodarone had no effect on contractility. Verapamil decreased contractility in a dose dependent manner, and all contractile colonies ceased to contract when 1×10^{-5} M verapamil was loaded. Procainamide and flecainide also decreased the beating frequency in a dose dependent manner. We also carried out β blocker loading in the presence of 1×10^{-6} M isoproterenol with cardiomyocytes derived from human iPS cells, which showed that contractility again decreased in a dose dependent manner under these conditions. There were no statistical differences between the drug concentrations required to elicit the effects in human iPS cells and those required to elicit the effects in cardiomyocytes derived from human ES cells (Fig. 4B). Previous reports have shown that some

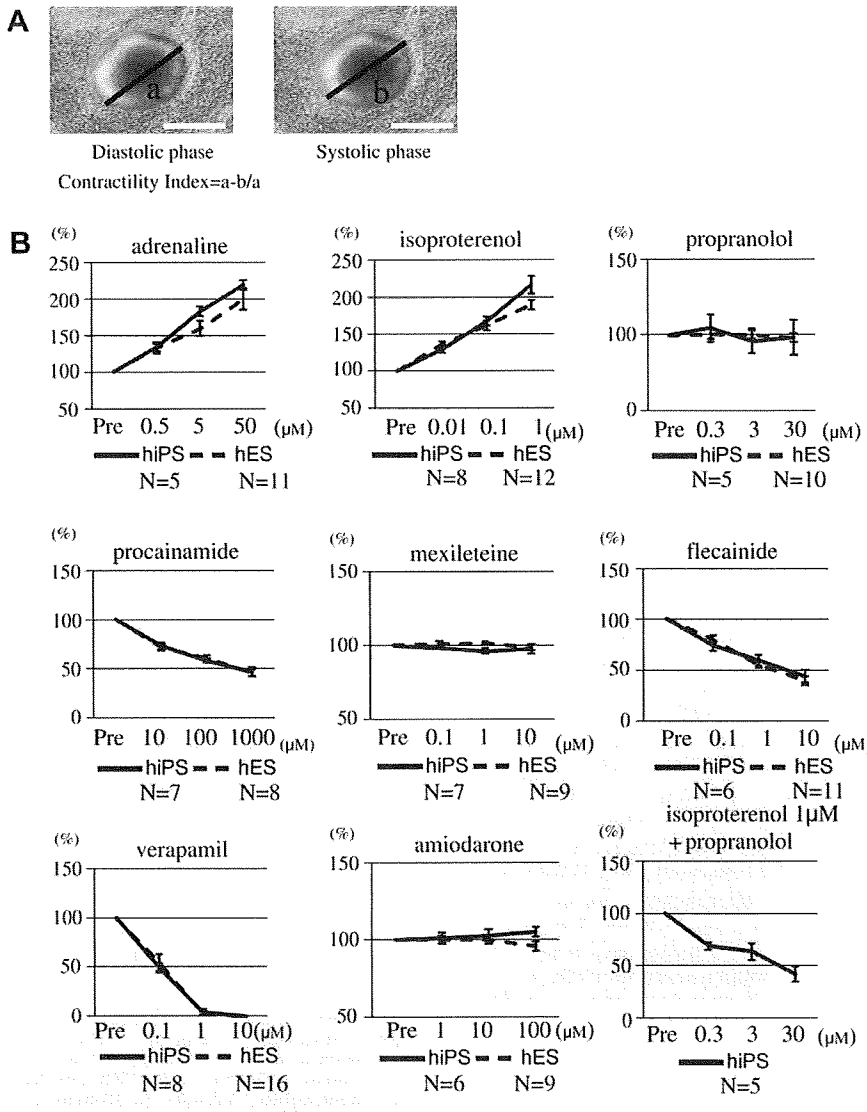

Fig. 4. Calculation of the contractility index. Right panel; diastolic phase, left panel; systolic phase. Scale bars = 200 μm (A). The effects of cardioactive drugs on the contractility of contractile colonies derived from human iPS cells and human ES cells. Adrenaline, isoproterenol, procainamide, flecainide, verapamil, and isoproterenol + propranolol had statistically significant effects on human iPS cells between pre-drug loading and the maximum concentration of the drug used in cardiomyocytes derived from human iPS cells ($P < 0.05$). There were no statistically significant differences between the concentrations of drugs that elicited effects in human iPS cells and those that elicited effects in human ES cells (B).

drugs had similar effects on the beating frequency of cardiomyocytes derived from ES cells and on *bone-fide* human cardiomyocytes, suggesting that human iPS cells and cardiomyocytes respond similarly to these drugs as well [12]. The results were compatible with clinical empirical results [15]. So we conclude that cardiomyocytes derived from human iPS cells respond similarly to drugs that affect contractility in human cardiomyocytes.

Table 1
Drugs and concentrations.

Class	Drugs	Concentration (M)
Na channel blocker	Procainamide	1×10^{-5}–1×10^{-3}
	Mexiletine	1×10^{-7}–1×10^{-5}
	Flecainide	1×10^{-7}–1×10^{-5}
β blocker	Propranolol	3×10^{-7}–3×10^{-5}
K channel blocker	Amiodarone	1×10^{-6}–1×10^{-4}
Ca channel blocker	Verapamil	1×10^{-7}–1×10^{-5}
α, β stimulant	Adrenaline	5×10^{-7}–5×10^{-5}
β stimulant	Isoproterenol	1×10^{-8}–1×10^{-6}

Table 2
Comparison with clinical empirical result.

Drugs	Result		Clinical efficacy	
	Contractility	Beating frequency	Contractility	Beating frequency
Procainamide	↓	→	↓	→
Mexiletine	→	→	→	→
Flecainide	↓	→	↓	→
Propranolol	↓	↓	↓	↓
Amiodarone	→	↓	→	↓
Verapamil	↓	↓	↓	↓
Isoproterenol	↑	↑	↑	↑
Adrenaline	↑	↑	↑	↑

Table 3
Primers for RT-PCR.

Genes	Direction	Sequence
Oct4 (endo)	Forward	GACAGGGGGAGGGGAGGAGCTAGG
	Reverse	CTTCCCTCCAACCAGTTGCCCCAAAC
Sox2 (endo)	Forward	GGGAAATGGGAGGGGTGCAAAAGAGG
	Reverse	TTGCGTGAGTGTGGATGGGATTGGTG
C-KIT	Forward	ATTCCCAGCCCATGAGTCCTTGA
	Reverse	ACACGTGGAACACCAACATCCT
Brachyury	Forward	AAGGTGGATCTTCAGGTAGC
	Reverse	CATCTCATTGGTGAGCTCC
KDR	Forward	AAAACCTTTTGTTGCTTTTGG
	Reverse	GAAATGGGATTGGTAAGGATG
Nkx2.5	Forward	GCGATTATGCAGCGTGCAATGAGT
	Reverse	AACATAAATACGGGTGGGTGCGTG
TBX5	Forward	AAATGAAACCCAGCATAGGAGCTGGC
	Reverse	ACACTCAGCCTCACATCTTACCCT
MEF2c	Forward	TTTAACACCGCCAGCGCTCTTCACCTTG
	Reverse	TCGTGGCGCGTGTGTTGTGGGTATCTCG
MLC2a	Forward	ACATCATCACCCACGGAGAAGAGA
	Reverse	ATTGGAACATGGCCTCTGGATGGA
MYHCB	Forward	CTGGAGGCCGAGCAGAAGCGCAACG
	Reverse	GTCCGCCCGCTCCTCTGCCTCATCC
HCN4	Forward	GGTGTCCATCAACAACATGG
	Reverse	TGTACTGCTCCACCTGCTTG
SCN5A	Forward	CCTAATCATCTTCCGCATCC
	Reverse	TGTTCATCTCTCTGTCCTCATC
Kir2.1	Forward	GACCTGGAGACGGACGAC
	Reverse	AGCCTGGAGTCTGTCAAAGTC
Kv4.3	Forward	GCCAGTCCCTGTGATTGTTT
	Reverse	CTCCATGCAGTTCTGCTCAA
HERG	Forward	TCCAGCGGCTGTACTCGGGC
	Reverse	TGGACCAGAAGTGGTCGGAGAACTC
CACNA1C	Forward	AACATCAACAACGCCAACAA
	Reverse	AGGGCAGGACTGTCTTCTGA
GAPDH	Forward	CACCAGGGCGCTTTTAACTCTG
	Reverse	ATGGTTCACACCCATGCGAAC

Discussion

In this report, we differentiated human iPS cells into cardiomyocytes, and compared the effects of drugs on cardiomyocytes derived from these cells and on cardiomyocytes derived from human ES cells, as well as with empirical results obtained in a clinical setting. The time course analysis of gene expression during cardiac differentiation was compatible to that seen during cardiogenesis of normal embryogenesis, and the results of the drug loading tests showed that cardiomyocytes derived from human iPS cells responded to drugs in much the same way as cardiomyocytes derived from human ES cells. The results were also compatible to empirical results obtained in a clinical setting.

Human iPS cells can be generated from somatic cell by introducing transcriptional factors. This technology is expected to generate patient-specific iPS cells suitable for the study of disease mechanisms, drug screening, and toxicology studies. This technology is easier to implement for the generation of patient-specific pluripotent cells than current technology which relies on nuclear transplantation technology to generate patient-specific pluripotent cells from ES cells. If cardiomyocytes derived from iPS cells could be shown to respond to drugs in the same way as human derived cardiomyocytes, then this technology would also constitute a major advance because it would allow the use of patient-specific iPS cell for the screening of patient-specific drugs against arrhythmic diseases, especially for lethal arrhythmic diseases such as LQTS where it is often very difficult to select for the best drug.

As the generation of cardiomyocytes from human iPS cells relies on the introduction of exogenous genes, we addressed the troublesome issue of whether cardiomyocytes derived from human iPS cells would respond to drugs in the same way as normal human cardiomyocytes. We considered the beating frequency and contractility to be very important indicators, because heart pump function is defined by beating frequency and contractility. So we investigated the effects of drugs on these two indicators, and found that drugs affect the beating frequency and contractility of cardiomyocytes derived from human iPS cells in much the same way as they do in a clinical setting. This result suggests that cardiomyocytes derived from human iPS cells could be used for drug screening tests instead of current screening procedures in a clinical setting. Cardiomyocytes derived from ES cells also responded to drugs in the same way as cardiomyocytes derived from human iPS cells.

Thus, these results suggest that patient-specific iPS cells could be used to select for the best drug to treat arrhythmic disease at the individual level, and would have the additional advantage of allowing the massive and rapid screening of drugs at concentrations that would be normally prohibitive in patients. However, until further studies are carried out, it is probably still too early to conclude that the drug effects on human iPS cell lines and patients are identical.

In conclusion, cardiomyocytes derived from human iPS cells have tremendous potential for drug screening, which should open the possibility of using patient-specific iPS cells in a clinical setting. The best drugs could be selected safely and rapidly by using human iPS cells from individual patients.

References

[1] A.J. Moss, J. McDonald, Unilateral cervicothoracic sympathetic ganglionectomy for the treatment of long QT interval syndrome, N. Engl. J. Med. 285 (1971) 903–904.
[2] A.J. Moss, P.J. Schwartz, R.S. Crampton, E. Locati, E. Carleen, The long QT syndrome: a prospective international study, Circulation 71 (1985) 17–21.
[3] M.C. Sanguinetti, C. Jiang, M.E. Curran, M.T. Keating, A mechanistic link between an inherited and an acquired cardiac arrhythmia: HERG encodes the IKr potassium channel, Cell 81 (1995) 299–307.
[4] Q. Wang, J. Shen, I. Splawski, D.L. Atkinson, Z.Z. Li, J.L. Robinson, A.J. Moss, J.A. Towbin, M.T. Keating, SCN5A mutations associated with an inherited cardiac arrhythmia, long QT syndrome, Cell 89 (1995) 805–811.
[5] I. Splawski, J. Shen, K.W. Timothy, M.H. Lehmann, S. Priori, J.L. Robinson, A.J. Moss, P.J. Schwartz, J.A. Towbin, G.H. Vincent, M.T. Keating, Spectrum of mutations in long-QT syndrome genes. KVLQT1, HERG, SCN5A, KCNE1, and KCNE2, Circulation 102 (2000) 1178–1185.
[6] I. Splawski, K.W. Timothy, L.M. Sharpe, N. Decher, P. Kumar, R. Bloise, C. Napolitano, P.J. Schwartz, R.M. Joseph, K. Condouris, H.T. Flusberg, S.G. Priori, M.C. Sanguinetti, M.T. Keating, Ca(V)1.2 calcium channel dysfunction causes a multisystem disorder including arrhythmia and autism, Cell 119 (2004) 19–31.
[7] P.J. Schwartz, S.G. Priori, C. Spazzolini, A.J. Moss, G.M. Vincent, C. Napolitano, I. Denjoy, P. Guicheneney, G. Breithardt, M.T. Keating, A.A. Wilde, L. Toivonen, W. Zareba, J.L. Robinson, K.W. Timothy, V. Corfield, D. Wattanasirichaigoon, C. Corbett, W. Haverkamp, E. Schulze-Bahr, M.H. Lehmann, K. Schwartz, P. Coumel, R. Bloise, Genotype–phenotype correlation in the long-QT syndrome: gene-specific triggers for life-threatening arrhythmias, Circulation 103 (2001) 89–95.
[8] D.J. Tester, L.B. Cronk, J.L. Carr, V. Schulz, B.A. Salisbury, R.S. Judson, M.J. Ackerman, Allelic dropout in long QT syndrome genetic testing: a possible mechanism underlying false-negative results, Heart Rhythm 3 (2006) 815–821.
[9] H. Vyas, J. Hejlik, M.J. Ackerman, Epinephrine QT stress testing in the evaluation of congenital long-QT syndrome: diagnostic accuracy of the paradoxical QT response, Circulation 113 (2006) 1385–1392.
[10] K. Takahashi, K. Tanabe, M. Ohnuki, M. Narita, T. Ichisaka, K. Tomoda, S. Yamanaka, Induction of pluripotent stem cells from adult human fibroblasts by defined factors, Cell 131 (2007) 861–872.
[11] I.H. Park, N. Arora, H. Huo, N. Maherali, T. Ahfeldt, A. Shimamura, M.W. Lensch, C. Cowan, K. Hochedlinger, G.Q. Dale, Disease-specific induced pluripotent stem cells, Cell 134 (2008) 877–886.
[12] J.Q. He, Y. Ma, Y. Lee, J.A. Thomson, T.J. Kamp, Human Embryonic stem cells develop into multiple types of cardiac myocytes, Circ. Res. 93 (2003) 32–39.

[13] M. Reppel, C. Boettinger, J. Hescheler, Beta-adrenergic and muscarinic modulation of human embryonic stem cell-derived cardiomyocytes, Cell. Physiol. Biochem. 14 (2004) 187–196.
[14] C. Xu, S. Polic, N. Rao, M.K. Carpenter, Characterization and enrichment of cardiomyocytes derived from human embryonic stem cells, Circ. Res. 91 (2002) 501–508.
[15] M.R. Rosen, Consequences of the Sicilian Gambit, Eur. Heart J. 16 (Suppl. G) (1995) 32–36.
[16] J. Hescheler, M. Halbach, U. Egert, H. Bohlen, B.K. Fleischmann, M. Reppel, Determination of electrical properties of ES cell-derived cardiomyocytes using MEAs, J. Electrocardiol. 37 (Suppl.) (2004) 110–116.
[17] M. Reppel, F. Pillekamp, K. Brockmeier, M. Matzkies, A. Bekcioglu, T. Lipke, F. Nquemo, H. Bonnemeier, J. Hescheler, The electrocardiogram of human embryonic stem cell derived cardiomyocytes, J. Electrocardiol. 38 (2005) 166–170.
[18] M. Reppel, P. Igelmund, U. Egert, F. Juchelka, J. Hescheler, I. Drobinskaya, Effect of cardioactive drugs on action potential generation and propagation in embryonic stem cell-derived cardiomyocytes, Cell. Physiol. Biochem. 19 (2007) 213–224.
[19] L. Yang, M.H. Soonpaa, A.D. Adler, T.K. Roepke, S.J. Kattman, M. Kennedy, M.E. Henckaerts, K. Bonham, G.W. Abbott, R.M. Linden, L.J. Field, G.M. Keller, Human cardiovascular progenitor cells develop from a KDR$^+$ embryonic-stem-cell-derived population, Nature 453 (2008) 524–528.
[20] W. Shimizu, C. Antzelevitch, Cellular basis for the ECG features of the LQT1 form of the long-QT syndrome, Circulation 98 (1998) 2314–2322.

Journal of Cellular Physiology

Orderly Hematopoietic Development of Induced Pluripotent Stem Cells via Flk-1$^+$ Hemoangiogenic Progenitors

AKIRA NIWA,[1,2] KATSUTSUGU UMEDA,[1] HSI CHANG,[1] MEGUMU SAITO,[1,2] KEISUKE OKITA,[3] KAZUTOSHI TAKAHASHI,[3] MASATO NAKAGAWA,[3,4] SHINYA YAMANAKA,[3,4] TATSUTOSHI NAKAHATA,[1,2] AND TOSHIO HEIKE[1]*

[1]*Department of Pediatrics, Graduate School of Medicine, Kyoto University, Kyoto, Japan*

[2]*Clinical Application Department, Center for iPS cell Research and Application (CiRA), Institute for Integrated Cell-Material Sciences, Kyoto University, Kyoto, Japan*

[3]*Basic Biology Department, Center for iPS cell Research and Application (CiRA), Institute for Integrated Cell-Material Sciences, Kyoto University, Kyoto, Japan*

[4]*Department of Stem Cell Biology, Institute for Frontier Medical Sciences, Kyoto University, Kyoto, Japan*

Induced pluripotent stem (iPS) cells, reprogrammed somatic cells with embryonic stem (ES) cell-like characteristics, are generated by the introduction of combinations of specific transcription factors. Little is known about the differentiation of iPS cells in vitro. Here we demonstrate that murine iPS cells produce various hematopoietic cell lineages when incubated on a layer of OP9 stromal cells. During this differentiation, iPS cells went through an intermediate stage consisting of progenitor cells that were positive for the early mesodermal marker Flk-1 and for the sequential expression of other genes that are associated with hematopoietic and endothelial development. Flk-1$^+$ cells differentiated into primitive and definitive hematopoietic cells, as well as into endothelial cells. Furthermore, Flk-1$^+$ populations contained common bilineage progenitors that could generate both hematopoietic and endothelial lineages from single cells. Our results demonstrate that iPS cell-derived cells, like ES cells, can follow a similar hematopoietic route to that seen in normal embryogenesis. This finding highlights the potential use of iPS cells in clinical areas such as regenerative medicine, disease investigation, and drug screening.
J. Cell. Physiol. 221: 367–377, 2009.

Because of their pluripotency and potential for self-renewal, embryonic stem (ES) cells have been used in various fields of science, including developmental biology (Evans and Kaufman, 1981). ES cells can differentiate into multiple cell types in a similar way to that observed in vivo. Previous studies using normal or gene-manipulated ES cells have helped to elucidate the process of normal embryogenesis and the genetic mechanisms of some diseases (Lensch and Daley, 2006).

Hematopoietic and endothelial development are regarded as particularly good processes for comparing the potential of ES cells cultivated in vitro with those grown in vivo (Nakano et al., 1994, 1996; Nishikawa et al., 1998). During embryogenesis, the developmental progression to a hematopoietic lineage is closely associated with progression to an endothelial lineage (Shalaby et al., 1997; Wood et al., 1997; Choi et al., 1998; Garcia-Porrero et al., 1998). Both cell lineages emerge from common mesodermal progenitors called hemangioblasts, which are positive for the vascular endothelial growth factor receptor Flk-1 (Flamme et al., 1995; Risau, 1995; Risau and Flamme, 1995; Choi et al., 1998; Huber et al., 2004). Thereafter, the site of hematopoiesis shifts from the yolk sac (primitive hematopoiesis) to the fetal liver, the spleen, and finally to the bone marrow (definitive hematopoiesis), and is accompanied by a change in the type of hemoglobin produced by erythrocytes (Moore and Metcalf, 1970; Matsuoka et al., 2001). Orderly hematopoietic development can be induced from murine and primate ES cells by various culture methods (Doetschman et al., 1985; Leder et al., 1985, 1992; Nakano et al., 1994, 1996; Xu et al., 2001; Umeda et al., 2004, 2006; Shinoda et al., 2007).

ES cells have been proposed as a potential new source of transplantable cells in regenerative medicine. It is anticipated that in the future such ES-derived cells may be used as sources of hematopoietic cells for stem cell transplants, or of mature blood cells for transfusion therapies. Recent studies have already shown that hematopoietic cells derived from murine ES cells overexpressing HoxB4 or Stat5 can replenish the bone marrow of lethally irradiated recipient mice (Kyba et al., 2002, 2003). However, there are various impediments to the clinical application of ES cells. For example, because they are established from the inner-cell masses of blastocysts, ES cells are subject to the controversy surrounding the manipulation of oocytes. Furthermore, the therapeutic use of ES cells from other individuals carries the risk of immunological complications.

Murine and human induced pluripotent stem (iPS) cells have recently been established from somatic cells by retrovirally introducing certain combinations of genes, such as octamer 3/4

The authors indicate no potential conflicts of interest.

Contract grant sponsor: Ministry of Education, Culture, Sports, Science, and Technology of Japan.

*Correspondence to: Toshio Heike, Department of Pediatrics, Graduate School of Medicine, Kyoto University, 54 Kawahara-cho, Shogoin, Sakyo-ku, Kyoto 606-8507, Japan.
E-mail: heike@kuhp.kyoto-u.ac.jp

Received 20 March 2009; Accepted 19 May 2009

Published online in Wiley InterScience (www.interscience.wiley.com.), 26 June 2009.
DOI: 10.1002/jcp.21864

(*Oct3/4*), sex-determining region Y-box 2 (*Sox2*), Krüppel-like factor 4 (*Klf4*), and the v-Myc avian myelocytomatosis viral oncogene homolog (*c-Myc*) (Takahashi and Yamanaka, 2006; Meissner et al., 2007; Okita et al., 2007; Park et al., 2007; Takahashi et al., 2007; Yu et al., 2007; Aoi et al., 2008; Hanna et al., 2008; Nakagawa et al., 2008). The cloned cells display properties of self-renewal and pluripotency similar to ES cells, and yield germ-line adult chimeras. However, because iPS cells are "unnatural" cells that are reprogrammed from once-differentiated cells, their differentiation processes must first be analyzed and compared before any true relationship between iPS and ES cells can be made.

The concept of patient-specific stem cells is of great clinical interest, and has engendered considerable research within the scientific community. The applications of these cells are expected to contribute to patient-oriented disease investigations, drug screenings, toxicology, and transplantation therapies (Jaenisch and Young, 2008). For example, a recent study demonstrated that autologous iPS cells can be used to treat mice with sickle cell anemia (Hanna et al., 2007). Despite such encouraging results, little is known about the in vitro hematopoietic differentiation of iPS cells. In particular, it is currently unclear whether iPS and undifferentiated embryonic cells follow the same process toward hematopoietic commitment.

In this study, we compared the hematopoietic differentiation of iPS and ES cells in vitro during their coculture with OP9 stromal cells (Nakano et al., 1994, 1996; Umeda et al., 2004, 2006; Vodyanik et al., 2005; Shinoda et al., 2007; Vodyanik and Slukvin, 2007). Sequential fluorescence-activated cell sorting (FACS), immunostaining, and reverse transcription (RT)-polymerase chain reaction (PCR) analyses demonstrated that iPS cell-derived hematopoietic and endothelial cells emerge from a common mesodermal progenitor that is positive for Flk-1, as is the case in ES cells and in normal embryogenesis.

Materials and Methods

Generation of iPS cells

Murine iPS cells were established from murine fibroblasts as described previously (Takahashi and Yamanaka, 2006; Okita et al., 2007; Nakagawa et al., 2008). In brief, to generate Nanog-iPS cells (clones 20D17, 38C2, and 38D2), murine embryonic fibroblasts carrying the Nanog-GFP-IRES-Puro^r reporter were incubated in retrovirus-containing supernatants for Oct3/4, Sox2, Klf4, and c-Myc for 24 h. After 2–3 weeks, clones were selected for expansion in medium containing 1.5 μg/ml of puromycin. To generate three-factor (without c-Myc) iPS cells (clone 256H18), murine tail tip fibroblasts (TTFs) were first isolated from adult *Discosoma* sp. red fluorescent protein (DsRed)-transgenic mice. Retrovirus containing supernatants for Oct3/4, Sox2, Klf4, and GFP were then added to the TTF cultures for 24 h. Four days after transduction, TTFs were replated on SIM mouse embryo-derived thioguanine and ouabain-resistant (STO)-derived feeder cells producing leukemia inhibitory factor (LIF; designated as SNL cells). Thirty days after transduction, the colonies were selected for expansion.

Maintenance of cells

The iPS cells and the murine ES cell line D3 were maintained on confluent SNL cells at a concentration of 1×10^4 cells/cm^2 in Dulbecco's modified Eagle's medium (DMEM; Sigma–Aldrich, St. Louis, MO), containing 15% fetal calf serum (FCS; Sigma–Aldrich) and 0.1 μM 2-mercaptoethanol (2ME) (Takahashi and Yamanaka, 2006; Okita et al., 2007; Nakagawa et al., 2008). OP9 stromal cells, which were a kind gift from Dr. Kodama (Osaka University, Osaka), were maintained as reported previously (Umeda et al., 2004).

Antibodies

The primary antibodies used for flow cytometric (FCM) analysis included an unconjugated anti-stage-specific mouse embryonic antigen (SSEA1) mouse monoclonal immunoglobulin M (IgM) antibody (sc-21702; Santa Cruz Biotechnology, Santa Cruz, CA), and the following anti-mouse antibodies from Becton–Dickinson (Franklin Lakes, NJ): unconjugated rat monoclonal anti-E-cadherin, rat monoclonal allophycocyanin (APC)-conjugated anti-c-kit, unconjugated rat monoclonal anti-spinocerebellar ataxia type 1 (Sca1), unconjugated rat monoclonal anti-CD31, biotin-conjugated anti-Flk-1, biotin-conjugated anti-CD34, and biotin-conjugated anti-CD45. Two secondary antibodies against the unlabeled primary antibodies were also from Becton–Dickinson: an APC-conjugated anti-mouse IgM antibody and an APC-conjugated anti-rat IgG antibody.

The primary antibodies used to immunostain the floating erythrocytes included rabbit anti-mouse embryonic hemoglobin (a gift from Dr. Atsumi, Miwa et al., 1991) and rat anti-mouse hemoglobin β (sc31116; Santa Cruz Biotechnology). Cy3-conjugated goat anti-rabbit or anti-rat antibodies (Jackson ImmunoResearch Laboratories, Inc., West Grove, PA) were used as secondary antibodies.

The primary antibodies for immunostaining endothelial cells included anti-mouse antibodies from BD (Becton–Dickinson), an unconjugated anti-VE-cadherin rat monoclonal antibody, an unconjugated anti-CD31 rat monoclonal antibody, and an anti-eNOS rat monoclonal antibody. Horseradish peroxidase (HRP)-conjugated goat anti-rat antibodies (Jackson ImmunoResearch Laboratories, Inc.) were used as secondary antibodies.

Cytostaining

Floating cells were centrifuged onto glass slides using a Shandon Cytospin® 4 Cytocentrifuge (Thermo, Pittsburgh, PA), and analyzed by microscopy after staining with May–Giemsa, myeloperoxidase (MPO), or acetylcholine esterase (Maherali et al., 2007). Staining was performed as described previously (Jackson, 1973; Yang et al., 1999; Xu et al., 2001). For immunofluorescence staining, cells fixed with 4% paraformaldehyde (PFA) were first permeabilized with phosphate-buffered saline (PBS) containing 5% skimmed milk (Becton–Dickinson) and 0.1% Triton X-100, and then incubated with primary antibodies against embryonic or β-major globins, followed by incubation with Cy3-conjugated secondary antibodies. Nuclei were counterstained with 4,6-diamidino-2-phenylindole (Sigma–Aldrich). Fluorescence was detected and images obtained with an AxioCam photomicroscope (Carl Zeiss Vision GmbH, Hallbergmoos, Germany).

FACS

The adherent cells were treated with 0.25% trypsin/ethylenediaminetetraacetic acid (EDTA) and harvested. They were incubated in a new tissue-culture dish (Becton–Dickinson) for 30 min to eliminate adherent OP9 cells (Suwabe et al., 1998). Floating cells were then collected and stained with primary antibodies, followed by incubation with APC-conjugated anti-mouse IgM or anti-rat IgG antibodies. Dead cells were excluded by propidium iodide (Kyba et al., 2002, 2003) staining. Samples were analyzed using a FACSCalibur and Cell Quest software (Becton–Dickinson). Cell sorting with the Flk-1 antibody was performed using a FACSVantage flow cytometer (Becton–Dickinson).

Differentiation of iPS and ES cells

For initial differentiation, iPS or ES cells were treated with 0.25% trypsin/EDTA (Gibco, Grand Island, NY) and transferred onto semi-confluent OP9 cell layers at a concentration of 6×10^3 cells/cm^2 in α-minimum essential medium (α-MEM;